MEDICAL ELECTRODE QUALIFICATION: PRELIMINARY DESIGN, INTEGRATION, AND VALIDATION OF THE TESTING SETUP

By

Alireza Ghasemi Ghodrat

Submitted in partial fulfilment of the requirements

for the degree of Master of Applied Science

At

Dalhousie University

Halifax, Nova Scotia

August 2022

Dedicated to

Whoever wants to make a positive footprint in this world

Table of Contents

List of Tables

List of Figures

Abstract

Over the past decades, researchers have been increasingly interested in developing and fabricating various new types of medical electrodes for the purpose of monitoring biopotentials or health signs. Among these electrodes, textile-embedded electrodes are the ones with the potential for long-term monitoring of health signs through the skin. In essence, textile-embedded electrodes are considered to be dry electrodes. They have conductivity hundreds to thousands of times lower compared to the available wet electrodes on the market. As a result, fabricating a highly conductive textile-embedded electrode, with essential characteristics such as durability, washability, and biocompatibility, would be beneficial. To that end, a systematic electrical conductivity testing setup for medical electrode qualification is a critical step in the design of experiments for fabricating new electrodes.

The scope of the current research is to design, fabricate, integrate, verify, and validate a preliminary testing setup based on the ANSI/AAMI EC12/2000/R2020 standard (the ANSI/AAMI standard) for medical electrode qualification in research laboratories. We verify and validate our unique testing setup as a robust starting point that simulates the interface between skin and market available electrodes with the hope that it might potentially be used to measures the electrical impedance of various novel fabricated medical electrodes in research laboratories in the future.

The focus of our investigations in this thesis is specifically on electrocardiography (ECG) measurement as the targeted biopotential. ECG was selected as it shows the overall condition and performance of a vital organ, the heart, in the body. Impedance was studied as a starting point for the electrical performance analysis of the medical electrodes in order to verify and validate the setup. The stability of the data produced by the setup was also investigated using an invariable stainless steel electrode. The results of the electrical performance of electrodes were compared together and statistical analysis were performed and interpreted. Overall, the current work shows that the integrated preliminary testing setup is a good starting point to further invest resources to develop more integrated features.

List Of Abbreviations Used

EEG: Electroencephalogram	FDA: Food and Drug Administration
ECG: Electrocardiogram	AC: Alternating current
EMG: Electromyogram	ANSI: The American National Standards Institute
ICFV: Intracellular fluid volume	AAMI: The Association for the Advancement of Medical Instrumentation
ECFV: Extracellular Fluid Volume	PVC: Polyvinyl chloride
ICF: Intracellular Fluid	PVDF: Polyvinylidene fluoride
ISFV: Interstitial Fluid Volume	IPA: Isopropyl alcohol
PV: Plasma Volume	DC: Direct Current

Acknowledgements

I would like to thank Dr. Ghada Koleilat for giving me the opportunity and trusting me to work on this project. This work was impossible without her continuous support over the past two years. Also, I would like to thank Dr. Sean Hinds for his invaluable insights over the past two semesters. Additionally, I am grateful to Dr. Paul Amyotte, and Dr. Robert Adamson, my committee members, for their constructive insights and help in my research. Special thanks go to the following parties and organizations including, but not limited to, Scotia Scholar Award, ResearchNS, MITACS, Lab2Market, IdeaHUB, Atlantic SpringBoard and AvisensX Inc., for their help in my research. I would like to acknowledge the research team – past, present, and future – for their support of research activities.

Last but not least, I would like to thank my family, my brother, Mehdi, and his wife, Asal, for their continuous support and love over the past years.

Chapter 1 – Introduction and Background

1.1.Preface

The scope of the current research is to redesign, integrate, and validate a testing setup based on the ANSI/AAMI standard for medical electrode qualification in research laboratories. Over the past decades, researchers have been increasingly interested in developing and fabricating various new types of medical electrodes for the purpose of monitoring biopotentials (health signs). Among these electrodes, textile-embedded electrodes have the potential for long-term monitoring of health signs from the human body. In essence, textile-embedded electrodes are considered dry electrodes. They have conductivity hundreds to thousands of times lower compared to the available wet electrodes on the market. As a result, fabricating a highly conductive textile-embedded electrode, besides including other essential characteristics such as durability, washability, and biocompatibility, would be beneficial.

To that end, a systematic testing setup for medical electrode qualification regarding their electrical conductivity is a critical step in the design of experiments for fabricating new electrodes. In other words, every new type of electrode has a variety of affecting parameters in its performance, including, but not limited to, the component and composition of materials, durability, biocompatibility and, more specifically, washability for textile-embedded electrodes. Understanding the effects of different parameters on electrical performance requires a systematic testing procedure. Additionally, developing new hardware requires much effort, including numerous trials and errors. Therefore, such a systematic and reliable testing system would help researchers to go through the trial and error procedures more effectively. Researchers could control various operational conditions and parameters except for one or two conditions and parameters currently under

investigation. Researchers could potentially figure out the optimum values for each parameter involved in the electrical performance of electrodes, leading to a practical product with the potential to be commercialized.

The focus of the current research is on ECG as the targeted biopotential and the electrical performance as one of the critical factors to be studied. ECG was selected because it shows the overall condition and performance of a vital organ, the heart, in the body. Additionally, impedance was studied as a starting point for the electrical performance analysis of medical electrodes. Appropriate experiments were designed to verify results produced by the testing setup. The testing setup was examined to verify that the data produced in each experiment could be repeated. As another part of the current research, the results were validated by the most similar prior work. Finally, conclusions and recommendations were presented.

1.2.Biopotentials

Biopotentials are generated from the volume conduction of currents made by collections of electrogenic cells. They are the generated bioelectrical signals of living cells and tissues of people and animals regardless of their activity. There are various types of biopotentials, including electroencephalogram (EEG), electrocardiogram (ECG), and electromyogram (EMG). Each of these biopotentials has its source of electrical signals. That is, each of these signals is generated by a specific organ or tissue in the human body. EEG, measured on the scalp, is the electrical potential induced by the collective activities of large numbers of neurons in the brain. ECG results from the action potentials of cardiac muscle cells, and EMG from contractions of skeletal muscle cells. Various other biopotentials (including but not limited to EOG, ERG, and EGG) also result from the collective effects of large numbers

of electrogenic cells or ionic distribution. These signals mirror the physiological state of their associated organs and can be considered reliable health indicators for clinical diagnosis and treatments (Bronzino, 2000; Ha et al., 2021; Kim et al., 2016; Oreggioni et al., 2019; Werner, 2014).

Capturing the required signals from these biopotential sources via electrodes is essential when physicians review their patients' medical conditions. A high-quality electrode is crucial when considering the patients' comfort level as well as adequate contact between the electrode and the skin. Therefore, electrodes have been designed and introduced over the past few decades to address problems with many of the currently available ones (Kim et al., 2016; Oreggioni et al., 2019; Sun & Yu, 2016).

One of the most important factors is the reliability of the performance of newly fabricated electrodes. Reliability, in essence, means the quality of being able to be trusted due to good performance, behavior, or work. Reliability in engineering fields is defined as a system or component's ability to function under specified conditions over a period of time (Cambridge University Press, 2022). In this context, reliability comes with repeatability; that is, the results from the targeted biopotential monitoring procedure should be similar under the same conditions. In the same way, the electrode performance over time and under similar operational conditions should be the same, eliminating the effect of the electrode performance interference on the result. If an electrode is not reliable and consistent in terms of its performance, that might lead to misleading results produced by machines interpreting the signals. The performance of the electrodes is defined based on specific parameters, including impedance, adhesiveness, and biocompatibility. Impedance is considered one of the most important electrical parameters in selecting electrodes (An & Stylios, 2018;

ANSI/AAMI, 2020; Bronzino, 2000; Oreggioni et al., 2019). Equation 1 demonstrates the simplified impedance formula based on the Ohm's law.

$$Z = \frac{V}{I}$$

Equation 1: Ohm's law – Impedance (Slurzberg, Morris; Osterheld, William, 1950)

Electrical impedance is a measurement of a circuit's or a component of a circuit's overall opposition to an electric current. Resistance and reactance are both included in impedance. Collisions of a current carrying charged particles with the conductor's interior structure cause the resistance component. The reactance component is caused by changing magnetic and electric fields in alternating current circuits, adding to the resistance to the flow of electric charge. In circuits carrying constant direct current, impedance becomes resistance. Based on Ohm's law, the higher the impedance (or resistance), the lower the current passing between two points (An & Stylios, 2018; Gross & Roppel, 2012; Macdonald, 1992).

Equation 2 shows the impedance for an ideal resistor. This equation explains that the impedance for an ideal resistor, which is called resistive impedance, is purely real. Equation 3 and Equation 4 demonstrate the correlations for the impedance of inductors and capacitors, respectively. Inductor and capacitor impedances construct the reactive impedance. According to Equation 3, the higher the frequency, the higher the inductor impedance. In contrast, the higher the frequency, the lower the capacitor impedance, based on Equation 4 (Gross & Roppel, 2012; Slurzberg, Morris; Osterheld, William, 1950).

$$Z_R = R$$

Equation 2: Impedance of a real resistor (Slurzberg, Morris; Osterheld, William, 1950)

$$Z_L = j\omega L$$

Equation 3: The impedance of inductors (Slurzberg, Morris; Osterheld, William, 1950)

$$Z_R = \frac{1}{j\omega C}$$

Equation 4: The impedance of capacitors (Slurzberg, Morris; Osterheld, William, 1950)

The mentioned impedance originates from different parts while capturing biopotentials. These parts can be summarized as follows: any tissue or organ underneath the epidermis, epidermis with the outermost layer, stratum corneum, as the main contributor to the overall impedance value, the electrode gel or sweat in between the skin/electrode interface, and the electrode (Tronstad et al., 2010; Werner, 2014; Jun Zhao et al., 2005). Researchers have proposed various models to illustrate the type of impedance for each part (An & Stylios, 2018; Heikenfeld et al., 2018; Laboratory, 1979). Figure 1 summarizes three of the models recommended by the researchers.

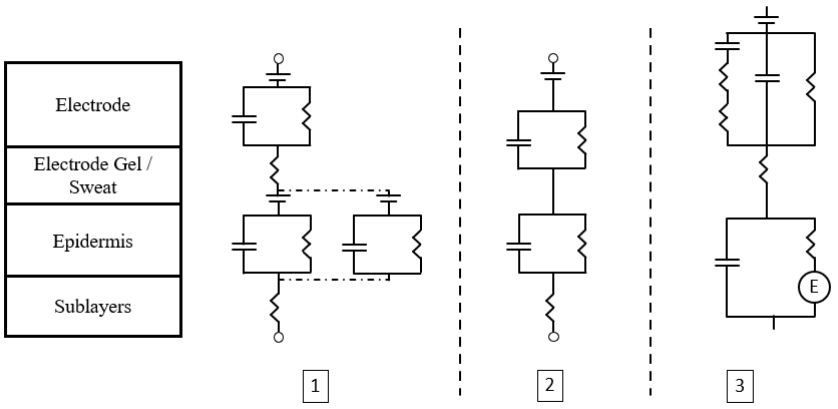

Figure 1: Three different models proposed by researchers for the skin-electrode interface – Model 1 (An & Stylios, 2018), Model 2 (Heikenfeld et al., 2018), and Model 3 (Laboratory, 1979)

Additionally, biopotentials deal with minimal amplitude ranges from tens to thousands of micro-volts (measured by surface electrodes). This range is at the bottom edge for ECG and EEG, meaning their amplitude ranges up to 100 mV. Ohm's law demonstrates a direct correlation between the voltage and the resistance, a direct correlation between current and voltage, and an indirect one between the current and the resistance. The intrinsic low ranges of amplitude and current for such biopotentials lead to a demand for a low impedance for the acquisition of electrical signals. That is, the overall impedance should be as low as possible between the source of the biopotential and the recording machine outside the human body. If impedance increases along the way, a more sophisticated amplifier will be needed to support the weak current. The electrodes are one of the significant sources of impedance. Currently, the Ag/AgCl electrodes have one of the lowest impedance values for biopotential monitoring, especially for ECG. Table 1 summarises the most common biopotentials, their applications, and the most common electrode types used to capture them

(Bronzino, 2000; Ha et al., 2021; Macay, 1963; Oreggioni et al., 2019; Park & Jayaraman, 2021).

Table 1: The most common biopotentials, their applications, and the recommended electrodes for monitoring (Macay, 1963; Oreggioni et al., 2019; Werner, 2014)

Biopotential/Bioelectric Signal	**Biological Source**	**Common Type of Electrode**
ECG/Electrocardiogram	Heart – as seen from the body surface	Ag/AgCl with sponge/hydrogel
EMG/Electromyogram	Muscle	Needle
EEG/Electroencephalogram	Brain	Gold cups Ag/AgCl Cups
EOG/Electrooptigram	Eye Dipole Field	Ag/AgCl with Hydrogel
ERG/Electroretinogram	Eye Retina	Thin fibre electrode
EGG/ Electrogastrogram	Stomach	Surface or needle electrodes
GSR/Galvanic Skin Reflex	Skin	Ag/AgCl with Gel

The mechanism behind the electrode/electrolyte interface can be summarized with the reactions shown in Figure 2. In this figure, C and A stand for cations and anions, respectively. These two reactions enable the flow of current through the electrode and electrolyte. In other words, it is the chemical reactions that enable the current flow through the electrode/electrolyte interface. A redox reaction will occur at the electrode/electrolyte interface. Assuming the electrode consists of the cations in the electrolyte, the electrode surface oxidation together with the coming anions to its surface results in the creation of a free electron in the electrode. The free electrons are then the building blocks of the passing current through the electrode/electrolyte interface (Bronzino, 2000).

$$C \leftrightarrow C^{n+} + ne^-$$

$$A^{m-} \leftrightarrow A + me^-$$

Figure 2: Electrode/Electrolyte interface reactions

Ag/AgCl electrodes are surface non-polarizable electrodes unlike the stainless steel ones. Such surface electrodes can be categorized as polarizable and non-polarizable. The major difference between these two types of electrodes can be summarized in how charges cross the electrode/electrolyte interface. In a polarizable electrode (e.g., stainless steel, platinum), the behaviour of the electrode is similar to a capacitor. This means that no actual charge crosses the interface. However, in a non-polarizable electrode (e.g., Ag/AgCl), the current crosses the interface freely with no required energy. Further in-depth explanation about these topics can be found in various references (Albulbul, 2016; Madhu, 2020).

1.1.1.Heart and the Associated Biopotential

Electrodes capture signals originating from the difference between the potential of inner and outer cell membrane sides, ranging from 50 to 100 mV. Various biopotentials' bandwidth varies from near zero to about 10000 Hz. For example, for ECG, the bandwidth, amplitude, and the number of signals would be 0.05-150 Hz, 100-15000 μV_{pp}, and 1-12, respectively. The number of signals refers to the number of leads; that is, there are 12 different signals associated with various parts of the heart muscles, which will define the activity performance of that part. Many heart problems can be diagnosed via the signals from each lead. In fact, every lead gives the physician a piece of information about the

heart status and performance. By combining all the pieces together, the physician gets a holistic understanding of the heart's physiological activity. For example, lead III might be a way to diagnose ischemia (i.e., impaired oxygen supply to the muscle) or infarction (damage to the muscle) on the left side of the chest. Further complementary information can be found in various references (Bronzino, 2000; Kim et al., 2016; Macay, 1963; Oreggioni et al., 2019; Thakor, 2014; Werner, 2014). Figure 3 illustrates the lead placement on the human body. As an example, lead III results from the placement of three electrodes on the left arm (LA), right arm (RA), and left leg (LL) and analyzing associated electrical signals.

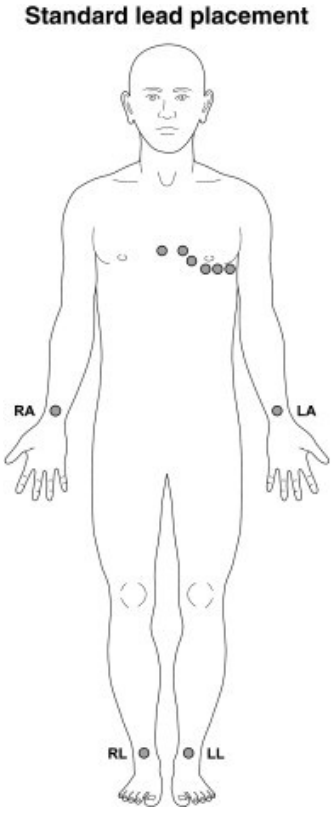

Figure 3: Left arm (LA) and right arm (RA) electrodes are placed on the left and right wrists. The leg electrodes (LL and RL) are placed on the left and right shins. The V1 chest electrode is placed to the right of the sternum in the fourth intercostal space. V (Reprinted with permission.) (Sheppard et al., 2011)

These limitations originate from the nature of the human body and are the limiting factors in the current experimental design. Equally important, the equipment capability and accessibility are the other limiting factors in the current experimental design. In addition, going beyond the mentioned limitations for the amplitude, frequency, or current while designing and conducting experiments is useless because the primary objective is to simulate the human body conditions.

In a human heart, a particular group of cells called node cells are responsible for controlling electrical pulses. The Sinoatrial (SA) node is responsible for the contraction of the upper heart chamber (atria) by generating an electrical signal. Then, after this signal passes

through the atrioventricular (AV) node, the lower heart chambers (ventricles) contract and pump blood through blood vessels. The SA node, also called the heart pacemaker, usually makes an adult human heart contract approximately 60 to 100 times per minute (Healthwise Staff, 2021).

The ECG signal acquisition is susceptible to biological interference, nearby muscle activities, and environmental noises. This susceptibility makes the selection of high-quality electrodes a vital consideration in this procedure. Table 2 summarizes noteworthy general features and problems associated with biopotentials. Choosing the right electrode for each of the mentioned biopotentials is a critical step in figuring out the correct status of the targeted organ. For electrodes, many factors play impactful roles in transferring the signal to the amplifier, including physical properties, such as the surface area, polarization, surface roughness, radius of curvature, and surface contamination (Bronzino, 2000; Macay, 1963; Malmivuo, 1995; Oreggioni et al., 2019; Thakor, 2014; Werner, 2014). Table 3 summarizes the correlations between the mentioned physical properties of electrodes and the associated correlations with the impedance.

Table 2: Noteworthy features and problems associated with biopotentials (Thakor, 2014)

Item	**Feature/Problem**	**Range/Description**
The most noteworthy features of biopotentials	Small amplitude	10 μV to 10 mV
	The low-frequency range of signals	Direct Current (DC) to several hundred hertz
The most noteworthy problems in biopotential acquisition	Presence of biological interference	skin, electrodes, motion, etc.
	Noise from environmental sources	power line, radio frequency, electromagnetic, etc.

These parameters are essential to consider when one is fabricating a new electrode. Optimizing the parameters based on their correlations with the resultant impedance is critical in fabricating a high-quality, low-impedance electrode using a cost-effective and time-efficient approach. These charges originate from the primary organ, e.g., the heart, and travel through body fluids up to the skin surface (Bronzino, 2000; Kim et al., 2016; Macay, 1963).

Table 3: Electrode effective physical properties and the associated correlations with impedance (Bronzino, 2000; Macay, 1963; Oreggioni et al., 2019)

Electrode physical property	**Change in the value**	**Impedance**	**Reason for the change in the impedance**
Surface area	Increase	Decrease	Allowance of more charges (current) to pass
Surface roughness	Increase	Decrease	Generally, increases the surface area; changes the wetting characteristics of a surface and significantly influences the dynamic contact angle during the droplet's interaction with the surface
The radius of curvature	Increase	Decrease	Closer to a flat surface structure, more contact area
Polarization	Increase	Increase	Imposes change in the charge distribution in the electrolytic solution adjacent to the electrode; induces the voltage change in the electrode leading to motion artifact in the measurement
Surface contamination	Increase	Increase	Contamination of electrode surfaces can result in severe polarization errors

1.2.Body Fluid

The distribution of the many fluid compartments in the body at the cellular level is critical for maintaining health, function, and survival. Water makes up 60% of a typical 70 kg man's entire body weight, which means 42 L. Intracellular fluid volume (ICFV) and extracellular fluid volume (ECFV) are the two primary compartments of the body's fluid. Twenty-eight of the 42 L of the water in the body is contained within the intracellular fluid (ICF) area. The interstitial fluid volume (ISFV) and the plasma volume (PV) make up the ECFV. The ECFV, comparable to 14 L, makes up one-third of the total body water. Seventy-five percent, or 10.5 litres, of the ECFV, presents in ISFV, with the rest in the PV. Table 4 explains the composition with generally associated concentrations of the extracellular fluid (Tobias et al., 2022).

Table 4: Extracellular fluid composition with the generally associated concentrations

Component	**Quantity (mEq/L)**
Sodium Na^{+}	136-145
Potassium K^{+}	3.5-5.5
Calcium Ca^{2+}	8.4-10.5
Chloride Cl^{-}	96-106
Hydrogen Carbonate HCO^{3-}	22-26

Plasma is primarily water (93 percent by volume). It contains dissolved proteins (fibrinogens, globulins, and albumins are the most common proteins), glucose, clotting factors, mineral ions (including but not limited to Na+, Ca++, Mg++, HCO3-, and Cl-), hormones, and carbon dioxide (plasma being the primary medium for excretory product transportation). These dissolved chemicals have a role in various physiological activities,

including gas exchange, immune system activity, and medication distribution (Tobias et al., 2022).

1.3.Electrodes

Electrodes for biopotential monitoring can be classified into three main categories: invasive microneedle electrodes, surface electrodes, and capacitive electrodes. Fu et al. have reviewed these types of electrodes comprehensively in their review article. The surface electrodes are the most promising of these three main categories with an acceptable contact impedance. The contact impedance of the invasive microneedle electrodes is even lower than that of traditional wet electrodes, making them the lowest contact impedance of dry electrodes. The stable skin-to-electrode contact interface produces a signal of a similar quality to that of wet electrodes. The length of microneedles must be appropriate to penetrate the stratum corneum of skin without breaking it or inflicting discomfort, which restricts the use of microneedle electrodes. However, penetrating the skin's stratum corneum raises the risk of infection. Additionally, because most microneedle electrodes are built on rigid substrates such as silicon and metallic materials, they are more vulnerable to motion distortions. Therefore, it is doubtful that dry electrodes would pursue the microneedle electrode as a future development path (Fu et al., 2020).

Similarly, capacitive electrodes face their types of complications in signal acquisition. According to Sun and Yu, the dry and capacitive electrodes could not attain a wet contact electrode's low impedance. Additionally, repeatable results are still anticipated. Although the capacitive electrodes do not need to be in direct contact with the skin, wearability must still be taken into account for comfort and long-term monitoring. The electrode design

appears to make a trade-off between comfort and steady monitoring. The unstable contact produces significant motion artifacts, which may be challenging to eliminate. They have the lowest performance among the mentioned electrode types because of lower electrical performance. One of their advantages is their being contactless while capturing the signals from the body; however, their success in being the dominant biopotential electrode type is unrealistic (Sun & Yu, 2016).

This means that not just one factor, such as electrical performance, would be the final reason to choose a type of electrode. Other factors, such as biocompatibility, durability, signal stability over time, and comfort level for the user, would be impactful in making the final decision. Out of these factors, electrical impedance is critical for electrodes in contact with the skin (Acar et al., 2019; An & Stylios, 2018; Nigusse et al., 2020).

1.4.Standards

Medical devices are required to be cleared by the health authorities in almost every country. Health authorities regulate these procedures and define the requirements and limitations for each classification or device type. Every medical device should pass a series of requirements defined and specified by such organizations. Medical electrodes are also considered medical devices that must be aligned with the requirements and limitations defined for them. A common type of such electrodes is the disposable ECG electrode. One of the globally recognized standards for this type of electrode was developed by the American National Standards Institute (ANSI) and the Association of Advancements in Medical Instrumentation (AAMI) (ANSI/AAMI, 2020; Laboratory, 1979).

The goal of the ANSI/AAMI standard is to establish minimum labelling, safety, and performance standards for disposable electrocardiographic (ECG) electrodes to ensure their safety and efficacy in clinical usage. The latest version of the AAMI standard includes additional standards for adhesive performance, coverage of all disposable electrodes, biocompatibility, and pre-attached lead wire safety. Also, it is worth mentioning that this standard does not cover the electrolyte composition requirements (ANSI/AAMI, 2020; Laboratory, 1979).

Unfortunately, copying and networking from the ANSI/AAMI standard are prohibited, though the licence was purchased from the provider. However, it was an attempt by the author to provide as much information as possible from the ANSI/AAMI standard for the audience, providing them with a vision of how the ANSI/AAMI standard was prepared and justified for its set limitations and requirements. Nevertheless, it is recommended that the reader refer to the original document as referenced here for further exploration of the mentioned topics (ANSI/AAMI, 2020).

The ANSI/AAMI standard attempts to establish a performance evaluation guideline for such medical devices. According to the ANSI/AAMI standard, the consequent misdiagnosis might substantially harm the patient's health if the device fails to appropriately transmit the electrical signal produced by the heart. The materials used in the device should fulfil a commonly recognised adequate degree of tissue compatibility because it is in direct contact with the skin. The device's capacity to sense and send an electrical signal should also be kept at a generally good level. A device design that enables significant interference from subject movement, or an incorrect electrode-medium combination that creates an overly high impedance, can create false diagnostic data. If the

physician uses erroneous diagnostic data to manage the patient, they may suggest a course of therapy that puts the patient in unnecessary danger (ANSI/AAMI, 2020; Laboratory, 1979).

Furthermore, the ANSI/AAMI standard explains the need for a consensus on the functional requirements essential to offer reasonable assurance of device safety and efficacy in clinical usage, and that is what spurred this initiative. The primary clinical risk addressed by the ANSI/AAMI standard is misdiagnosing a patient's condition due to inaccurate electrocardiographic data transmission. However, the standards should not be seen as rigid or unchanging. The ANSI/AAMI standard must be upgraded to suit new needs based on technological advancements and understanding, as in any industry (ANSI/AAMI, 2020; Laboratory, 1979).

1.4.1.Electrical Impedance Requirements

According to the ANSI/AAMI standard , a two kΩ maximum impedance value was set for the average value of 10 Hz impedance for 12 electrode pairs connected gel-to-gel with an impressed current lower than 100 μA. The two kΩ level is a compromise that guarantees the user a minimal likelihood of interference issues brought on by the electrode while also allowing for design flexibility for the electrode. For electrodes used in most stationary monitoring applications, where preparation is limited, a five kΩ limit would be appropriate. Different Alternating Current (AC) impedance limitations for various applications were deemed unworkable. Thus, the committee decided to use the lowest number as the overall limit. The committee also considered the fact that ECG monitors have protection

mechanisms built-in to absorb overloads induced by defibrillation and electrosurgery current (ANSI/AAMI, 2020; Laboratory, 1979).

Moreover, the ANSI/AAMI standard explains that the AC impedance requirement is provided as a mean value and an allowable upper limit for quality assurance. Cables and/or monitors have current-limiting resistors built into them to absorb these excess currents and the energy they produce. Suppose the electrode's resistance contributes significantly to the current-limiting protection resistances. In that case, a significant quantity of heat might be created at the skin/electrode contact, increasing the risk of electrode failure and patient damage (ANSI/AAMI, 2020; Laboratory, 1979).

Furthermore, the ANSI/AAMI standard clarifies that while the 1-Hz impedance is essential for ECG integrity, the ANSI/AAMI standard stipulates that measuring impedance at 10 Hz has become an industry standard. It was clarified that this requirement was set due to the challenges faced while determining the 1-Hz impedance using generally available equipment. In other words, setting the 1 Hz frequency requirement for measuring impedance is impractical. However, in another section, it was mentioned that the working group considered measuring electrode impedance at 1 Hz during the development of this standard edition, and the working committee made the final decision. Furthermore, the fact that commercially marketed electrodes work adequately supports the 10-Hz measurement's suitability as a predictor of electrode performance (ANSI/AAMI, 2020; Laboratory, 1979).

In this research, a testing setup was redesigned and integrated based on Model 1, illustrated in Figure 1. The testing setup was designed to be able to follow the ANSI/AAMI standard requirements and simulate a few human physiological conditions, including but not limited to body temperature and pressure, sweat and body fluid compositions, the frequency,

amplitude, and current value ranges of targeted biopotentials, the outmost layer of the human skin, and sweat secretion. Out of the mentioned conditions, a frequency range for ECG monitoring based on the human heart frequency range was set into the testing setup. Additionally, the ionic environment of the body was simulated using a salt solution with a defined concentration. The membrane was used to simulate the skin pore size with the ability to transfer ions from both sides. The current research was unable to simulate body temperature and pressure. The skin is a complicated organ, and simulating it needs more efforts.

The focus of the current research is on ECG as the targeted biopotential and the electrical performance as one of the critical factors to be studied. ECG was selected because it shows the overall condition and performance of a vital organ, the heart, in the body. Additionally, impedance was studied as a starting point for the electrical performance analysis of medical electrodes. Appropriate experiments were designed to investigate the verifiability of the results produced by the testing setup. In other words, the testing setup was examined to verify the repeatability of the data produced in each experiment. As another part of the current research, the results were validated by the most similar prior work. Finally, errors and their root causes were summarized together with possible recommendations for future work.

Chapter 2 – Problem Statement and Motivation

2.1.Current Research Objective

Choosing the right electrode for biopotential monitoring depends on various factors, including but not limited to electrical performance, labelling, patch quality and design, safety, price, and biocompatibility. Each of these factors must pass specific requirements and follow a series of limitations set by health authorities before entering the market. As one of these factors, electrical performance, which is a part of this research, has its requirements and limitations depending on the targeted biopotential.

In this research, the focus is on ECG as the targeted biopotential and the electrical performance as one of the critical factors to be studied. ECG was selected because it states the overall condition and performance of a vital organ, the heart, in the body. Furthermore, the leading cause of death for men and women is due to heart disease. Additionally, impedance was studied as a starting point for the electrical performance analysis of medical electrodes. This property is one of the most critical electrical properties for ECG monitoring.

Every electrode for monitoring biopotentials needs to be cleared to enter the market by the health authorities. The requirements and limitations in different countries vary, making it more difficult, complicated, and time-consuming to get final clearance. Medical electrodes are considered medical devices that must follow specified standards, limitations, and requirements. The American National Standards Institute (ANSI) and The Association for the Advancement of Medical Instrumentation (AAMI) developed standards for disposable ECG electrodes (ANSI/AAMI, 2020).

These types of electrodes are considered class II, because they are neither life-supporting nor life-sustaining but are potentially hazardous to life or health even when properly used (Laboratory, 1979).

The ANSI/AAMI standard (ANSI/AAMI, 2020) scope was defined as below:

> "This standard contains minimum labeling, safety, and performance requirements; test methods; and terminology for disposable electrocardiographic (ECG) electrodes. (p. 3)"

The ANSI/AAMI standard covers various topics related to disposable ECG electrodes, including requirements and tests for labeling, packaging, safety, biological response, adhesive performance, and electrical performance. Looking at the electrical performance section, which is the focus of the current research, one can understand that there is no systematic, in-detail explanation of how to conduct the electrical performance tests. The section in the ANSI/AAMI standard specifies a circuit model, the environmental conditions, the electrical parameters, limitations, and requirements for the test results, but not how to conduct the tests systematically. To make it more straightforward, the ANSI/AAMI standard proposes two general methods of doing the electrical performance test, either by attaching a pair of electrodes to specified spots on the human body and performing the measurements, or attaching a pair of electrodes with some electrode gel in between them and connecting them to measurement devices (ANSI/AAMi, 2020; Laboratory, 1979). Both methods have their limitations. The human body artifacts will affect the measurements, as was mentioned earlier. Additionally, attaching two electrodes is a non-systematic and limiting framework because, for example, it would not be possible to study sweat composition and secretion rate. Furthermore, testing medical devices on

humans, or better to say, any human/clinical trial, includes extensive, time-consuming, bureaucratic, and ethical procedures that might be costly for research groups and their projects.

Research and development centers are the backbones of delivering new technologies and innovations (Saboo, 2017). Research centers focusing on developing new technologies for biopotential monitoring are no exception. High-quality and reliable products result from systematic product development through which researchers have assessed various impactful parameters and conditions. By searching through the most recent (2022) literature on biopotential electrode fabrication (Based & Lectrodes, 2022; Dong et al., 2022; Eskandarian et al., 2022; Maithani et al., 2022; Schauss, 2022; Wang et al., 2022; Jingjing Zhao et al., 2022), it can be concluded that the research laboratories' testing procedure is still based on voluntary participation (Figure 4). This way of assessing the electrical performance of newly fabricated electrodes is too complicated because of uncontrolled parameters, including sweat composition and secretion rate, the thickness of the skin and the selected area on the body to capture the electrical signal, and general body condition. As a result, a fundamental understanding is missing of different parameters and conditions' effects on the electrode electrical performance through a repeatable, reproducible, and reliable method based on the available standards (Westbroek et al., 2006).

Figure 4: An example of how research centers test their newly fabricated electrodes (reused with permission © 2022 IEEE) (Teferra et al., 2022)

These limitations suggested the below question and motivated the author to provide an answer for it: Is there any systematic way of assessing the electrical performance of the newly fabricated electrodes in research laboratories under human physiological conditions? In other words, what should one do if they are developing a new medical electrode in a research laboratory and are interested in evaluating the electrical performance of the new electrode considering the standards, limitations, and requirements? The motivation here is to find, design, and validate a testing setup that could be further upgraded and adopted in research labs worldwide.

The current research is one preliminary objective toward the mentioned goal. It is to design, integrate, validate, and verify a testing setup as a starting point to simulate an ionic transfer environment for testing the electrical impedance of newly fabricated medical electrodes in

research laboratories. Furthermore, the objective is to conduct a comparative analysis of the data from testing the newly fabricated electrodes under environmental and technical conditions mentioned by the standards.

2.2.Prior Research

Priniotakis et al. (2005) developed an electrochemical cell to test the quality of newly fabricated electrodes. This cell was made up of two electrodes that were planarly placed next to one another and supported by a Polyvinyl Chloride (PVC) tube and two PVC plates. Special membranes that closely resemble human skin were positioned between the electrodes and the electrolyte. The work aimed to analyze and comprehend the behavior of textile electrodes. Furthermore, researchers were interested in obtaining a better understanding of the interphases between electrode-electrolyte and electrode-skin-electrolyte to model the system and use it to monitor parameter and body conditions. Measuring the human body's behavior over the sweat secretion period under this simulated environment was another value of their work (Priniotakis et al., 2005).

In another attempt, Westbroek et al. (2006), applied a similar concept to evaluate and monitor the performance of electrodes composed of conductive knit, woven, and non-woven textiles. They used artificial sweat containing 20 grams per liter of NaCl, 1 gram per liter of urea, 500 milligrams per liter of other salts, and NaOH or HCl as the pH controller to maintain the value at 5.8. The cell consists of 4 PVC plates with the electrodes positioned between the outer and inner plates. A hole within the two inner plates was designed to hold the electrolyte and to allow contact between the electrodes from both ends. The applied alternating potential had a frequency range of 1 mHz to 1 MHz and a maximum

amplitude of 10 mV. Their results showed interesting application possibilities under various environments to investigate the behaviour of newly developed electrodes with the possibility of monitoring several parameters, including heart rate, respiration rate, and biopotential readings, without many mistakes (Westbroek et al., 2006).

In 2018, An and Stylios applied the same concept to test the newly fabricated textile electrodes and compare the electrical performance with a commercially available one. This attempt was made to measure the skin-electrode impedance without the presence of unwanted impedance variations induced by human skin. A PVC tube secured with Polyvinylidene Fluoride (PVDF) membranes from both sides was used to hold the 0.9% NaCl solution as the electrolyte. The orientation of the cell was vertical with the reference electrode, the commercially available Ag/AgCl electrode at the bottom and the new electrode at the top. Further explanations of their work will be discussed in chapter four of this thesis (An & Stylios, 2018).

Chapter 3 – Methodology and Experimental Design

3.1.Introduction

This chapter reviews the testing setup's design, integration, validation, and verification process. The design of the testing setup (instrument), its components, and the chemical materials used are detailed herein. The integration of the system components is described as well as how they all work together. The methodology and verification process is presented to show the verifiability of the results generated by the instrument. Finally, the results are compared with the most similar prior research for the purpose of validation.

Designing and building a new instrument both take trial and error. The current research is no exception, and it took months to understand the correct procedures. Figure 5 shows the step-by-step progression of how the instrument was designed and built. We first defined the problem and then set specific objectives to achieve. The next step was to brainstorm how to tackle the challenges by designing the experiment and understanding the various parameters and conditions involved in the experiment. Gathering and analyzing the data were also significant steps to interpret the validity of our system. Finally, by having the results and comparing them to the primary objective, necessary modifications were applied, starting again from the brainstorming step. This trial-and-error procedure continued until the objectives were successfully achieved.

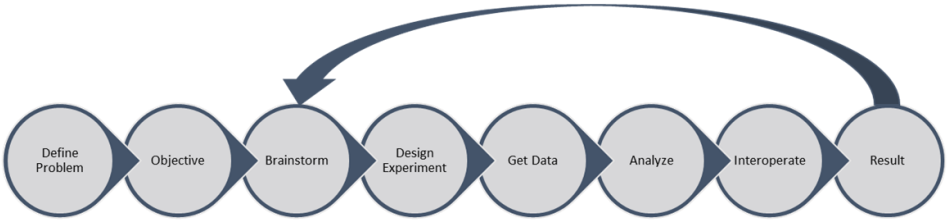

Figure 5: Procedure to design the instrument

Figure 6 shows the first version of the instrument built. This design was used to better understand each component's process and configuration. The procedure took a couple of months before we started the design and integration of the next upgraded version that addressed our requirements.

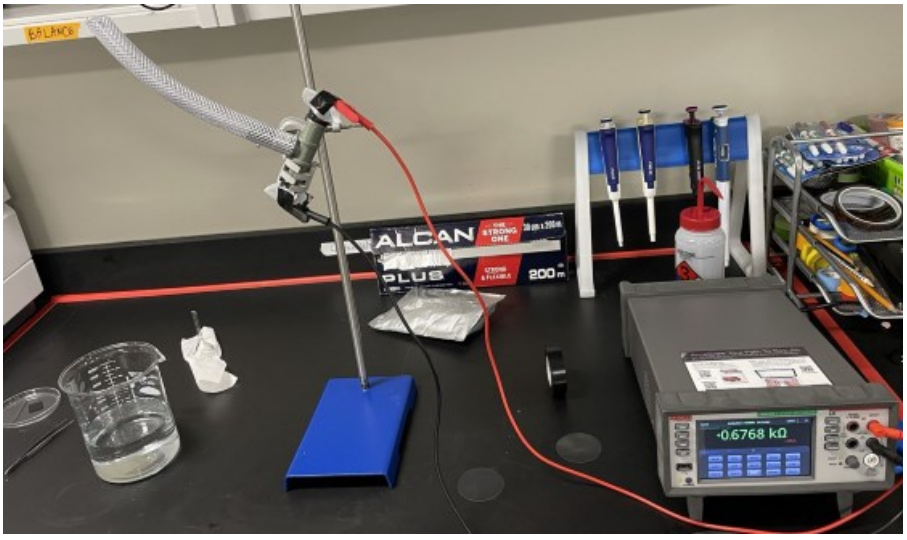

Figure 6: Testing setup (instrument) – first version

Figure 7 and Figure 8 show a schematic design of the instrument and the integrated setup in the laboratory. The instrument consists of four major parts: the PVC chamber, membranes, electrodes, and the measurement unit (LCR meter). A three-way PVC chamber (chamber) was used for the ionic transfer medium. As seen in Figure 9, on each of the two far ends of the chamber, 10 cm of a Double-Sided Mounting Tape, specifically 3M 5925 VHB Heavy Duty Foam Tape 2" (Tape), was applied to affix two permeable hydrophilic PVDF membranes. The 47 mm diameter membranes had a 0.1 µm pore size and were purchased from Sigma (Figure 10). Electrical measurements were conducted using a HIOKI General-Purpose LCR Meter with measurement frequencies of Direct Current (DC), and from 4 Hz to 8 MHz (Figure 11). The LCR meter was connected to the instrument using a test fixture (Figure 12) and a pair of wires made in the laboratory (Figure 13). The salt solution was prepared using sodium chloride (purchased from Sigma) and deionized (DI) water.

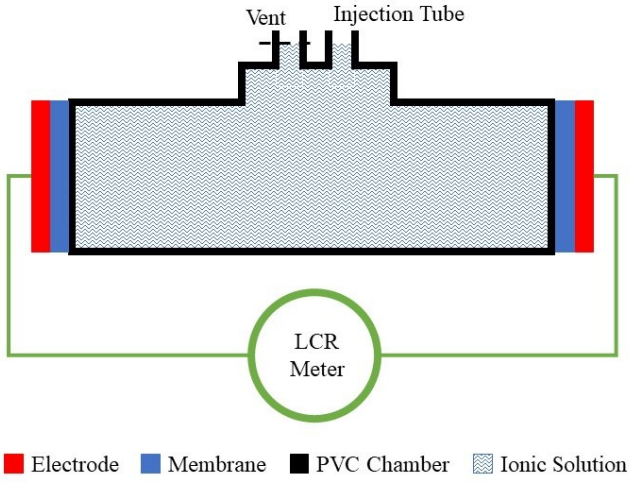

Figure 7: Schematic design of the testing setup (instrument)

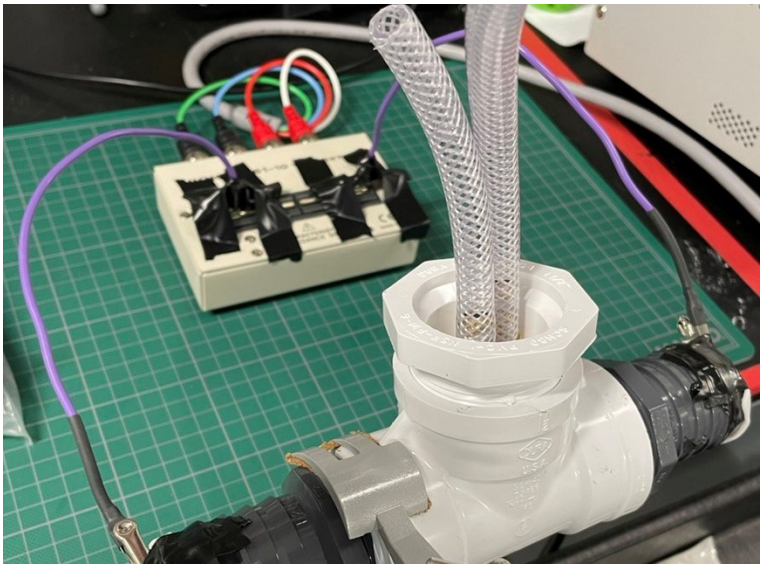

Figure 8: Testing setup (instrument) – second version

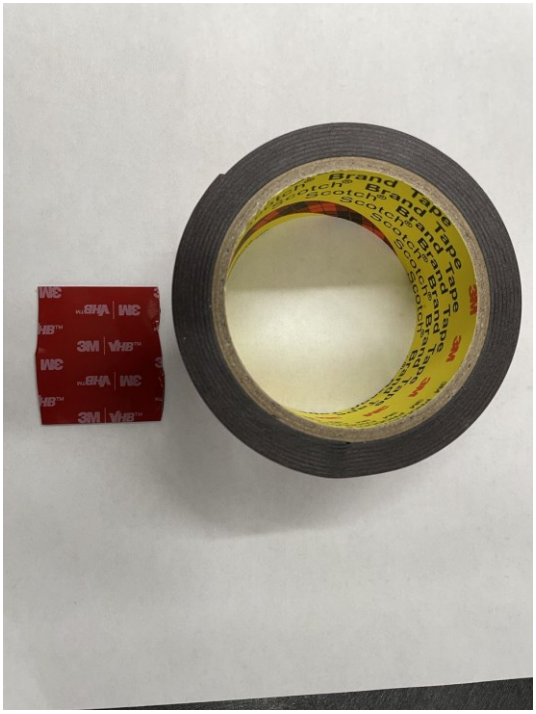

Figure 9: 3M Heavy Duty Foam Tape

Figure 10: Membrane

Figure 11: LCR meter – HIOKI IM 3536

Figure 12: Test fixture for the LCR meter

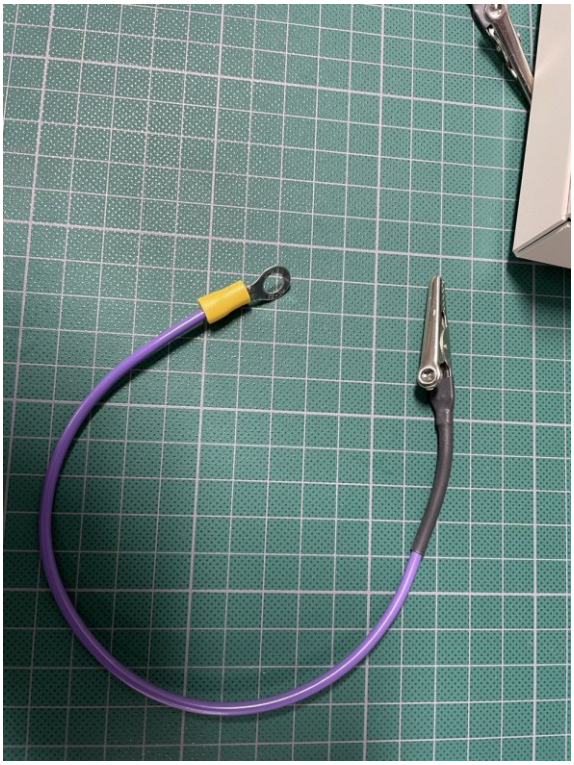

Figure 13: Wire connectors between the test fixture and the instrument

In order to have a reliable wire connection between the test fixture and the electrodes being applied to the membranes, a special wire connector (Figure 13) was made in the laboratory. This new wire connector was used instead of regular alligator clips to accommodate the structure of the test fixture and electrodes. Additionally, the whole cylinder was designed horizontally to make sure the fluid pressure on the membranes on both sides was balanced. Furthermore, two inlets, one for vent and the other one for fluid injection/removal, were designed for the chamber. The vent allowed the air to be removed from the chamber and replaced by fluid. Also, this design had the ability to apply pressure generated by the fluid head to the membranes from inside the chamber, to study the effect of body fluid pressure on electrical performance. This capability could enable us in the future to investigate the effect of various fluid compositions on the electrical performance of electrodes.

The edges of the chamber were cleaned using Isopropyl alcohol (IPA) and then with DI water to ensure the surface was ready for the tape to be applied. Afterward, the tape was applied to both far-end inlets of the chamber to fully cover the entrances. The tape on top of each entrance was cut to leave a circular hole on each entrance with taped edges of 3 mm. Afterward, the membranes were placed on top of each taped entrance. The membranes were double-checked to ensure they were fully attached to the taped area around both entrances. Finally, the membranes were secured around the entrances with black electrical tape.

On both sides and on top of the membranes, electrodes were applied. Various electrodes, including 3M 2570 RedDot hydrogel (Figure 14), 3M 2249-50 RedDot sponge (Figure 15), 3M 2248-50 sponge (Figure 16), and 3M 2231 RedDot sponge (Figure 17), were purchased for running the experiment and verifying the testing setup. Before attaching the electrodes

onto the membranes, 0.25 ml of a conductive gel purchased from Signa Gel (Figure 18) was applied on top of the center of the conductive parts of the electrodes. After attaching the electrodes to the membranes, the specially prepared alligator clips (Figure 13) were connected to the snap button of the electrodes. The connection area was fastened using black electrical tape. Two 10 cm lengths of tape were used to protect the connection area. Afterward, the alligators were connected to the LCR for data acquisition.

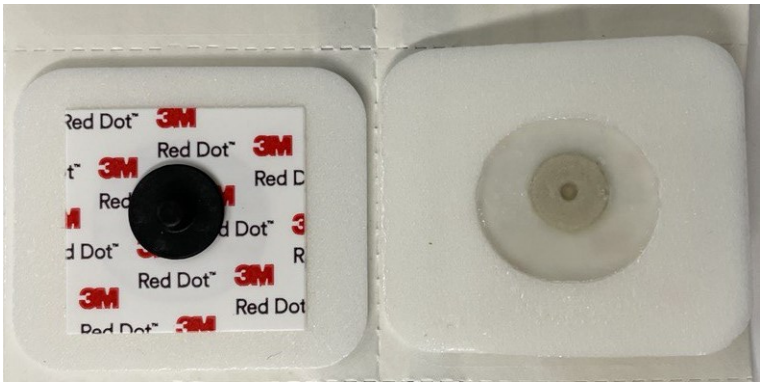

Figure 14: 3M RedDot 2570 ECG electrode - Ag/AgCl with sponge

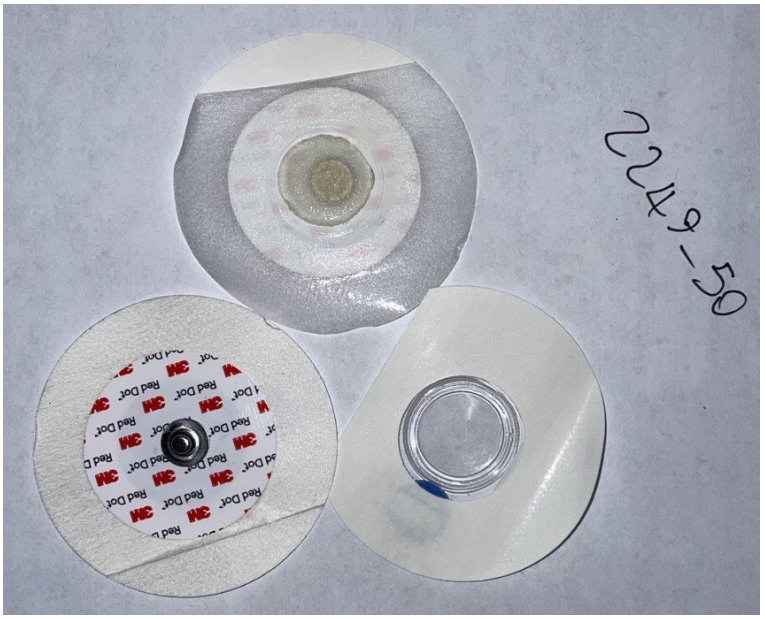

Figure 15: 3M RedDot 2249-50 ECG electrode - Ag/AgCl with sponge

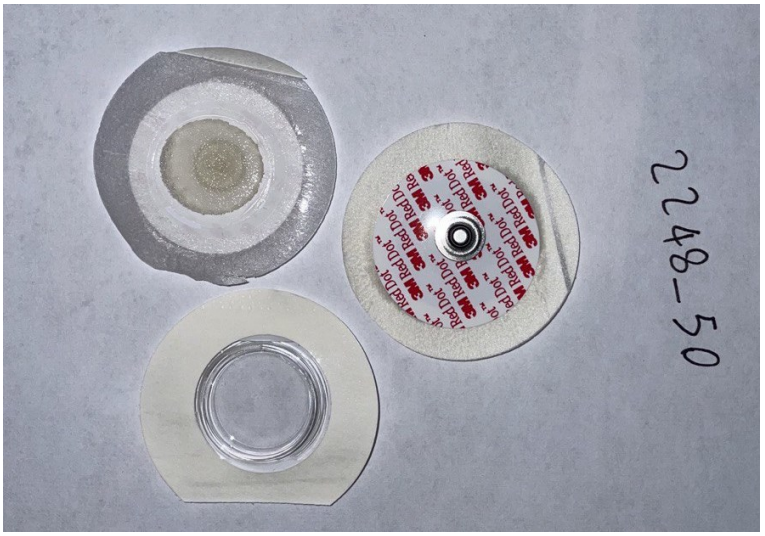

Figure 16: 3M RedDot 2248-50 ECG electrode - Ag/AgCl with sponge

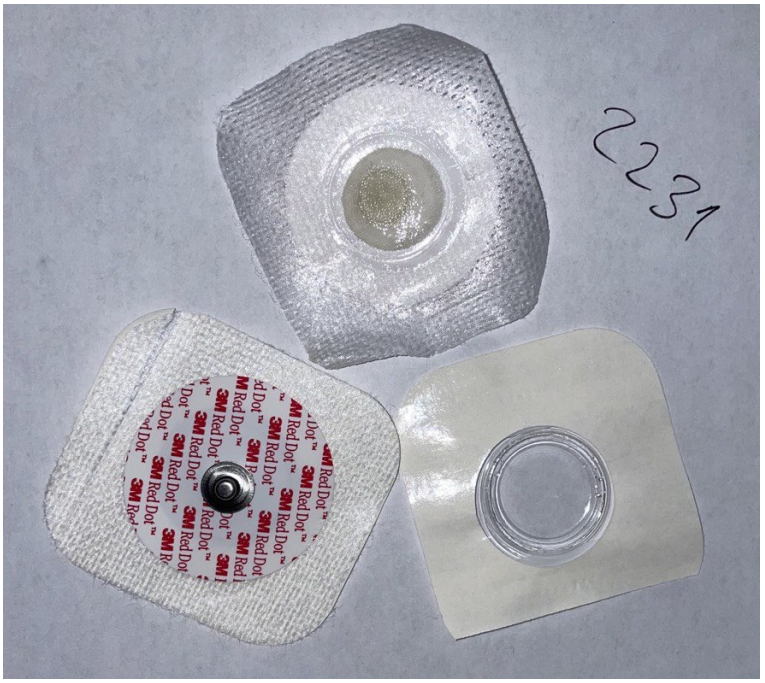

Figure 17: 3M RedDot 2231 ECG electrode - Ag/AgCl with sponge

Figure 18: Electrode Gel

Two stainless steel electrodes (provided by an industry partner) were used to evaluate the stability of results produced by the instrument (an electrochemical cell). Figure 19 shows the stainless steel electrodes used for this experiment. Before using the stainless steel electrodes, they were pretreated physically and chemically to avoid the effects of dirt, contamination, or surface roughness on the electrical signals.

To this end, the electrodes were polished using nail emery. They were then washed with soap to clean dirt and grease from the surfaces. Next, IPA was used as a promising sterilization tool, ensuring the surfaces were free of microorganisms (*Isopropyl Alcohol As A Cleaning Agent*, 2021). Then, the electrodes were washed with acetone to remove any dirt or organic substances from the surfaces (Industrial Deegreasers, 2018). All steps took 30 seconds to be completed. DI water was used between each step to clean residues.

Figure 19: Stainless steel electrode

Stainless steel was chosen because of its durability and resistivity against corrosiveness. Prior research used pure Palladium as electrodes for characterizing their electrochemical cells. Palladium is one of the noble metals with specific properties. Resistivity to oxidation and corrosion in moist air is one of the properties of noble metals. Likewise, stainless steel has the same properties in terms of resistivity and corrosiveness. As a result, considering our resource limitations, stainless steel electrodes were chosen for the current experiment.

This step helped us understand if the electrochemical cell, the main component of the instrument, provided constant stable connectivity between the electrodes. It was an attempt to ensure that any fluctuation in the resultant impedance from any new electrode was due to the nature of the electrodes themselves, not influenced by the electrochemical cell. The preparation procedure to run the experiment with stainless steel electrodes was the same as other procedures except for when electrode gel was used. In that case, the electrode gel was first applied to membranes and spread across membranes uniformly. Figure 20 illustrates the instrument while running the experiment.

The LCR machine comes with software (Figure 21) to run and control experiments remotely from a desktop computer. Using the sweep measurement (Figure 22) capability in the software, data was acquired under specific electrical conditions.

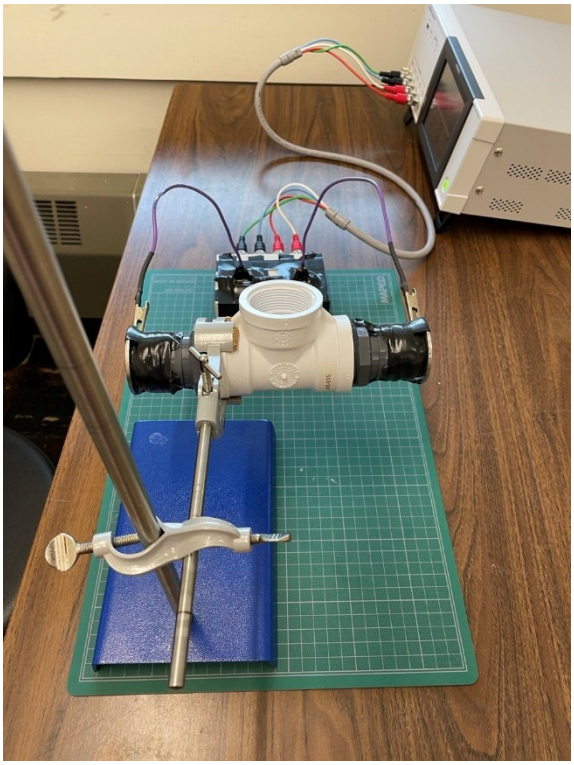

Figure 20: Instrument - characterizing the electrochemical cell

Before starting the experiment, the LCR machine needed to be calibrated. Calibration was done based on the procedures described in the manual provided by the vendor (HIOKI). Calibration was done in four steps. First, the LCR machine was turned on with the test fixture, and all the wires were connected. The machine was left for 60 minutes to warm up before doing the next two steps. Secondly, the length of the test fixture cable plus the alligator connectors was entered into the calibration setting panel in the machine interface. Thirdly, the open circuit mode was run by keeping the alligators apart from each other by the length of the chamber. Finally, the short circuit mode was run by attaching the alligators to each other.

The sweep measurement was done using the HIOKI software. To do so, the following steps were followed. The LCR machine was connected to the computer using the USB cable. After running the software on the computer, the USB port was selected, and the LCR button was clicked. A message popped up asking the user whether to erase the calibration setting on the machine. The user did not erase the local setting on the machine. Afterward, four possible parameters were selected on the software's user interface. For the current research, the impedance, the angular phase, the resistance in parallel, and the capacitance in parallel were chosen to be measured, though the impedance would be the only focus for the current research's statistical analysis. Then, the sweep measurement option was chosen from the drop-down menu (Figure 22). It should be noted that the mentioned steps for the software may be changed if the vendor makes any updates.

Within the sweep measurement window, under the sweep point section, the frequencies at which the user intends to measure the electrical parameters were entered like a column of numbers. Frequency was selected as the sweep mode. The interval between sweep point, the number of measurements, and the interval between measurements were selected as 0, 2880, and 30, respectively, for the current research. The overall time of the experiment was 24 hours, equivalent to 2880 measurements within 30 seconds of time intervals. It should be noted that the machine does not consider the time it takes to capture the data. This increases the total time of the experiments depending on the number of frequencies used to acquire data. For the current research, the total run time for each experiment was almost 31 hours. It is recommended to select the checkboxes related to the acquisition of voltage/current together with the one for instrument setting. Finally, the user clicked the start measuring button, which was followed by a pop-up window, asking the user to choose

the name and location of the output file for the measurements. At the end of the measurements, a pop-up window announced the end of the experiment.

Subsequently, the required electrical conditions for the experiment were defined in the LCR desktop software. These conditions included the frequency range (4 to 120 Hz with a one-unit increment for each measurement), the total time of the experiment (24 hours excluding the time needed for the instrument to capture data within the mentioned frequency), and the time interval between each measurement (30 seconds). Table 5 shows a summary of the primary parameters used for the experiments.

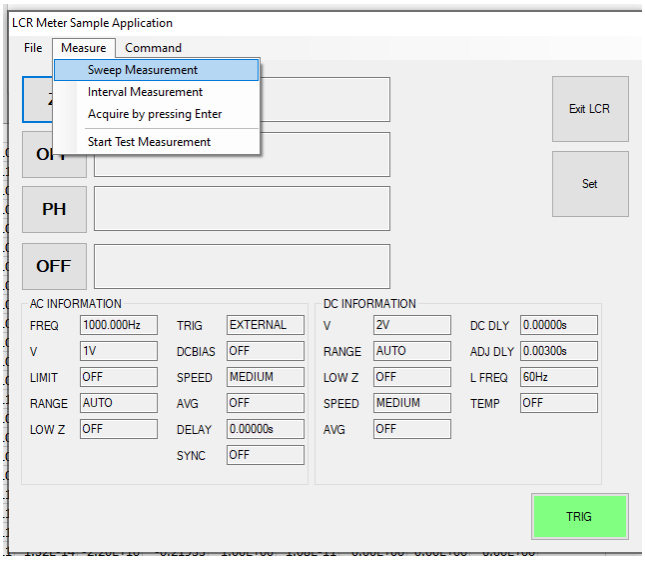

Figure 21: LCR meter software

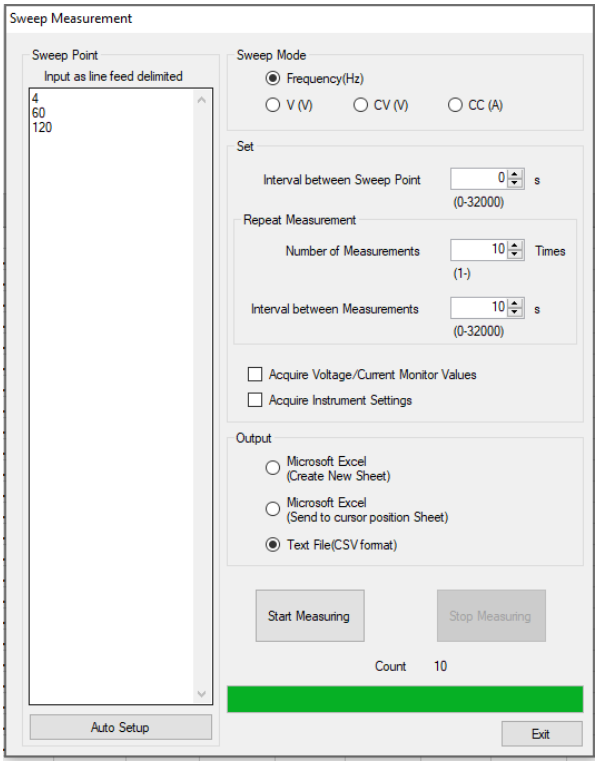

Figure 22: Sweep measurement

Figure 23 describes the sweep measurement procedure and the associated time intervals using an LCR meter. The waiting time between each measurement was 30 seconds. The measurement each time took about 8 seconds. Therefore, the total time of the experiment extended to 31 hours rather than the originally planned 24 hours.

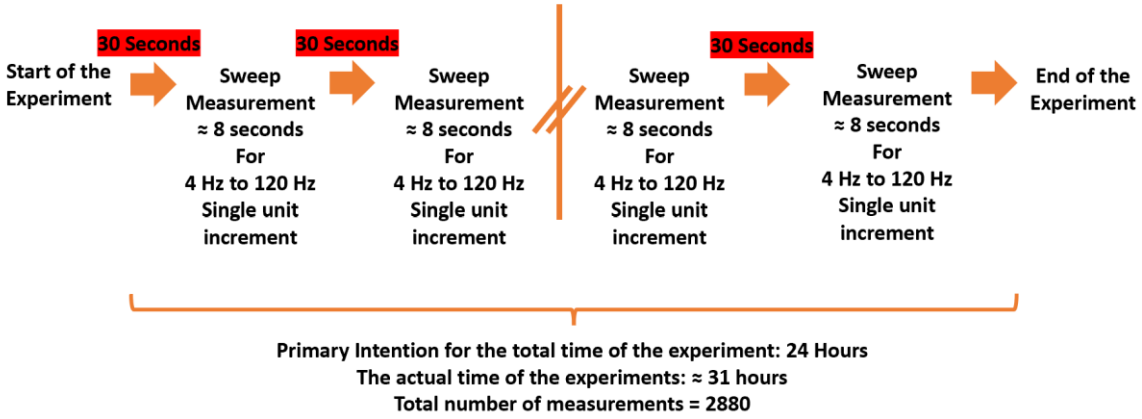

Figure 23: Sweep measurement procedure using LCR

The solution inside the chamber was 0.9% NaCl. This concentration was chosen due to its similarity to the amount of salinity in human body fluid and sweat. The solution was prepared by dissolving 2.25 grams of NaCl into 250 ml of DI water, using a volumetric flask.

Table 5: Primary parameters for the experiments

Item	Range/Quantity
Frequency	4 Hz to 120 Hz (1 unit increment)
Voltage	< 1 V
Current	< 6 mA
Chamber capacity	250 ml
Membrane pore size	0.1 micrometer
Conductive Gel	Signa Gel (Electrode Gel)
Electrode	Ag/AgCl with hydrogel Ag/AgCl with sponge Stainless Steel
Active Surface Area (Ag/AgCl) Active Surface Area (Stainless Steel)	78 mm^2 706 mm^2
Duration	24 hrs
Measurement internals	30 Seconds
Ambient temperature (°C)	22 ± 5
Humidity (%)	40 ± 10

3.2.Verification and Stability

Every instrument and instrumentation process needs to be verified. Verification in this context means the ability of the instrument to produce repeatable data. Repeatability is one of the key characteristics of a verified instrument and the associated instrumentation process. In this research, the author's attempt was to conduct an experimental design under specified environmental conditions and parameters to verify the instrument. In this section, the verification process will be explained.

Table 6 shows the parameters and environmental conditions when the experiments were conducted. The frequency range for the sweep measurements was 4 Hz to 120 Hz with one-unit increments. The total experiment time was 24 hours with measuring intervals of 30 seconds. The LCR machine does not count the time it takes to acquire the data from the

instrument; that is, the total time of each experiment exceeded from the original 24 hours to around 31 hours. All experiments' AC voltage and current were below one volt and 6 microamperes, respectively. The total capacity of the chamber for the ionic solution was 250 ml. The laboratory's temperature and humidity experienced a fluctuation within the range of 22 ± 5 ℃ and 40 ± 10 %. Seven experiments were conducted over the course of 11 days.

Each experiment took approximately 31 hours, including preparing and dismantling the instrument. All parameters and environmental conditions were kept the same as much as possible. For all experiments in the verification phase, one type of electrode, 2570 3M RedDot hydrogel, was used. In each experiment, the membranes, the sealing, the electrodes, the ionic solution, the electrode gel, and the tapes were changed to a new one. To minimize the effect of human error, the location of the device, the calibration, and the wire connection were kept the same for the 11 days of experiments. Proper spacing between the LCR machine and the surrounding area was considered to help air circulation and cooling purposes. After all the experiments, the results were saved for further analysis. Furthermore, the stability test of the electrochemical cell was done by the stainless steel electrodes. All parameters and conditions were the same as described in Table 6.

Table 6: Experimental design parameters for the instrument verification

Item	Range/Quantity
Frequency	4 Hz to 120 Hz (1 unit increment)
Voltage	< 1 V
Current	< 6 mA
Chamber capacity	250 ml
Membrane pore size	0.1 micrometer
Conductive Gel	Signa Gel (Electrode Gel)
Electrode	Ag/AgCl with hydrogel Stainless Steel
Active Surface Area (Ag/AgCl) Active Surface Area (Stainless Steel)	78 mm^2 706 mm^2
Duration	24 hrs
Measurement intervals	30 Seconds
Ambient temperature (°C)	22 ± 5
Humidity (%)	40 ± 10
Number of experiments	7

As mentioned earlier in this document, impedance is among the most important electrical parameter to study for biopotential monitoring and instrumentation. As different electrodes might have various surface areas, impedance - defined as the impedance over the cross-section area of the electrode in contact with the membrane to carry the charges - is considered the main electrical parameter to investigate in the current research. The number of experiments and days for the purpose of verification were limited due to the time-intensive nature of the system experiments and the limitations on scheduling the booking of shared laboratory space within COVID safety restrictions. Experiments required the entire laboratory to be reserved and secured for at least 32 hours per experiment conducted. As other researchers were working in the same space and using the same equipment, running more experiments was not possible. As a result, it should be noted that more

experiments are recommended to investigate the repeatability of the data for the next upgrade of the instrument. Aside from the number of experiments, the same procedure, operator, equipment, environmental conditions, location, and item or unit under test must be adopted to run repeatability tests (Hogan, 2018).

3.3.Validation

After verifying the instrument, the results must be validated by prior published research. In other words, to ensure that the results generated by the instrument were reliable, they needed to be validated by either similar prior publication or fundamental science. The author tried to verify the research outcomes using either of the mentioned sources.

3.4.Data Analysis

Sufficient statistical analysis is a key step in experimental design. Research dealing with a huge number of data sets need to be analyzed carefully; it is important to disregard unnecessary data from the primary data cloud. In this research, the author attempted to extract valuable data regarding the scope of his thesis objective, provide a better understanding of the generated data, interpret, define the meaning of final results, and provide conclusions following recommendations as well as root causes of errors for the instrument. Within the verification process, which consisted of more than a million data sets, various hypothesis and Q-tests for the presence of an outlier were performed. Other descriptive statistical works will be presented in the next chapter.

3.4.1.Normal Distribution

As a significant step in the current research, the data distribution was analysed to determine whether they follow a normal distribution pattern. In this case, the empirical rule for the normal distribution was used as the criteria to determine whether a distribution is normally distributed or not. Based on the empirical rule for normal distributions, if 68%, 95%, and 99.7% of data is within one, two, and three standard deviations from the mean, respectively, the data distribution is considered as normally distributed (Frost, 2022).

3.4.2.Q-test

An outlier is an observable potential deviation from the rest of the results or samples. An experiment that has been run incorrectly may lead to an outlier. An incorrect result may erroneously affect the final conclusions from the experiments. For example, a potential outlier can reject the repeatability of data produced by an instrument, whereas the instrument is in reality producing repeatable data. This means we are missing an actual event, even due to the lack of tools to determine the potential outliers. To this end, Dixon's Q test was used to determine possible outliers. This test was done on a small number of observations or sample sizes (usually less than 10). The distribution has to be normally distributed, and the test should be used only once for each set of data. Dixon's Q test is a quick and popular test for outlier detection in a few fields, including chemistry (Rorabacher, 1991). The associated procedure on how to conduct the test in a dataset is as follows:

Data were sorted in ascending order. The potential outlier data point was selected. Equation 5 shows the general formula for the test. In this formula, gap refers to the difference

between the potential outlier data point to its closest data point, whereas the range denotes the difference between the maximum and minimum data points of the distribution (Raschka, 2014).

$$Q = \frac{|Gap|}{|Range|}$$

Equation 5: Dixon's Q test Formula

The significance level for the seven data points was considered 90% in this research. The critical Q value was obtained using the significance level and available tables in the literature (Rorabacher, 1991). Based on the tables, the associated critical Q value for this research was 0.507. The targeted data point was considered an outlier if the calculated Q was bigger than the critical Q value. In other words, the result of each Q test was whether or not the targeted data point was an outlier. This test was conducted for all 2880 datasets obtained throughout the entire runtime.

3.4.3. Hypothesis test for the potential outliers

Once the results from all Q tests for 2880 datasets were obtained, a hypothesis test was conducted to determine whether the entire associated curve, consisting of the targeted data points, could be an outlier. To this end, the null hypothesis was "The associated curve is not an outlier." The significance level was considered 95%, meaning that the null hypothesis is rejected if at least 95% of the Q test results from the 2880 tests were outlier.

Otherwise, the alternative hypothesis, "The associated curve is an outlier," would be true, and the null hypothesis would be rejected.

3.4.4. F-test

F-test was performed on two data sets, the Ag/AgCl 2570 and stainless steel electrodes. The purpose of this test is to find out whether or not the instrument can distinguish between different electrodes and if successful, we can state with certainty that the system is functioning as it is supposed to. The significance level for the F-test is taken at 5%. The test was simply performed in Office Excel. The test was repeated with a sample of 1000 datapoints taken from the end of experiments to compare the variances at the point where both electrodes have stabilized.

The null hypothesis for these tests is "There is no difference between the variance of both electrodes." The alternative hypothesis is "Ag/AgCl electrode has a higher variance for impedance compared to stainless steel electrode." The normally distributed results of experiments are also aligned with the F-test requirements.

Chapter 4 – Results and Discussions

This chapter presents the results of the conducted experiments in addition to the interpretation of the obtained results. Chapter 4 explains the rationale behind every step taken to provide clear answers to the questions posed earlier in the thesis. We first present the results of the verification experiments followed by a thorough statistical analysis followed by results interpretations. Afterwards, we compare the electrodes and discuss the value of such instrumentation process. Finally, the results were validated by comparing our results to published research.

4.1.Verification

The verification process consists of two parts: the first is conducting the experiment with testing the repeatability of the data being generated by the instrument through seven experiments under the exact same operational conditions, and the second is testing a stainless steel electrode to verify the stability of the ionic environment for data acquisition.

Figure 24 shows the results of the experiments from the verification phase. The vertical and horizontal axes denote the impedance in Ohm, and the time in minutes, respectively. From the figure, it can be observed that all curves follow almost the same pattern, starting with an approximately 2% decrease in the value of their impedance followed by approximately 45% increase in that value and stabilizing through a polynomial manner. This manner, with its negative associated kurtosis value determined in Table 7, shows a lower likelihood of extreme events.

Out of the seven curves in Figure 24, an outlier Q-test was performed for the farthest curve (3rd). Alpha was considered 0.1, and the number of data points for each Q-test was 7. There were 2880 measurements for each experiment over the entire runtime. As a result, 2880 was the number of times a Q-test was performed for the 3rd curve.

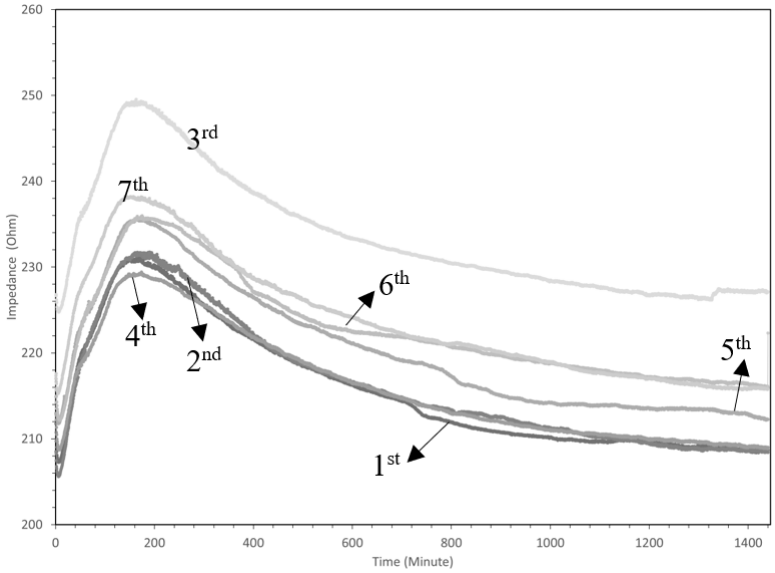

Figure 24: Impedance over time - verification phase (raw data from the seven experiments)

Afterward, the hypothesis test was conducted for the 3rd curve consisting of the targeted potential outlier data points (Figure 25). This test investigates the entire curve, which consists of 2880 datapoint measured for the 3rd experiment and determines whether or not the entire curve is an outlier. The significance level was considered at 5%. This is the most common significance level to consider as for a preliminary stage of such instrumentation process. To this end, the null hypothesis was "The associated curve is not an outlier." The null hypothesis would be rejected if at least 95% of the Q-test results from the 2,880 tests were outliers. Otherwise, the alternative hypothesis, "The associated curve is an outlier,"

would be true, and the null hypothesis could be rejected. This means that if 2736 of the Q-tests considered the selected curve data points as outliers, the whole curve would be an outlier. In this case, 2413 of the Q-tests resulted in an outlier, meaning the selected curve was not considered an outlier. Therefore, the null hypothesis could not be rejected.

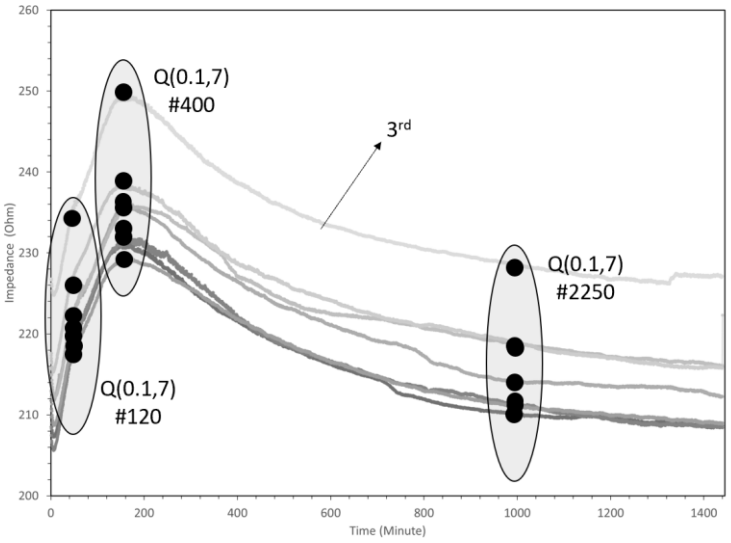

Figure 25: Schematic procedure of the Q test for the entire datasets

Table 7 demonstrates various statistical analysis results regarding the seven experiments. The mean was chosen as the representative of the seven experiments for future comparative analysis. Out of the experiments, the lowest and the highest mean were 215.79 and 233.51. The mean as the average representative of the data points will consider the effect of skewness, unlike the median and mode.

The objective with conducting these above experiments is to observe the resultant curves and investigate how similar they are relative to each other. The system was prepared in the

exact same fashion for all experiments; meaning that any inaccuracy or error in the system or any delay in having a saturated membrane exists for all experiments. This similarity can be tested by looking at the descriptive statistics provided in Table 7. Such statistical tools as the mean, standard deviation explain the centrality and data dispersion, respectively. By looking at not only the mean and standard deviation of the resultant curves, but also the median, range, minimum, maximum, skewness, kurtosis, and the largest and smallest amounts, the similarity of results and curves are understandable. For instance, the range for all curves is somewhere between 20.73 to 26.13, with 23.74 as the mean. To elaborate further, the objective here is to see the curves with descriptive statistics as close as possible. Table 7 presents the descriptive statistic for the reader to better understand the associated curves.

Table 7: Descriptive statistics for the seven experiments

Statistical Tool	**2570 (1st)**	**2570 (2nd)**	**2570 (3rd)**	**2570 (4th)**	**2570 (5th)**	**2570 (6th)**	**2570 (7th)**	**Difference**
Mean	215.79	216.34	233.51	216.09	220.28	222.74	223.72	8%
Standard Error	0.13	0.13	0.13	0.12	0.13	0.11	0.13	0%
Median	212.66	213.79	231.1	213.82	218.55	221.23	221.58	9%
Mode	209.9	231.03	227.25	211.43	213.96	216.96	215.86	10%
Standard Deviation	7.03	7.21	6.87	6.39	7.13	6.01	6.85	3%
Sample Variance	49.39	51.93	47.23	40.77	50.82	36.08	46.91	5%
Kurtosis	-0.72	-0.67	-0.38	-0.85	-0.76	-0.45	-0.69	-
Skewness	0.79	0.77	0.91	0.7	0.73	0.83	0.72	-
Range	23.86	26.13	24.79	20.73	23.93	23.81	22.97	4%
Minimum	207.26	205.61	224.77	208.7	211.75	212.16	215.26	8%
Maximum	231.12	231.74	249.56	229.43	235.68	235.97	238.22	8%
Sum	621478.2	623070.76	672521.96	622344.25	634410.14	641500.73	644310.35	8%
Count	2880	2880	2880	2880	2880	2880	2880	-
Largest	231.12	231.74	249.56	229.43	235.68	235.97	238.22	8%
Smallest	207.26	205.61	224.77	208.7	211.75	212.16	215.26	8%
Confidence Level (95.0%)	0.26	0.26	0.25	0.23	0.26	0.22	0.25	-

The last column in Table 7 shows the difference percentage betweeen the highest and lowest number for its associated statistical tool relative to the lowest. The difference in standard deviation between the highest and lowest value among all experiments is 3%. Considering the 10% significance level for the basic statistical tools such as mean, and standard deviation, the instrument produce simlar results from the same type of electrode in multiple experiments. This reflects the repeatability of the instrument in procuding simlar consistent results from experiments following the exact operational conditions. It should be noted that the significance level is a subjective criterion and is selected based on the nature of the experiments and conditions observed by the researcher. This significance level can be changed and reduced for the future upgraded versions of the instrument.

A slight difference can be observed between the seven curves, meaning they were not an exact fit for each other. In order to be able to comparatively analyze the performance of this particular electrode with other ones, the mean of the seven experiments was chosen.

Though there might be a few options, the mean average curve was chosen as the representative of the seven experiments for comparative analysis. Additionally, Figure 26 illustrates the normalized curved relative to the mean of the seven experiments. Normalizing all seven curves relative to the mean gives us a sense of how far they are from the mean. All experiment results except the third one are within 5% of the resultant mean. Likewise, the results of seven experiments can be observed within a 95% confidence interval around the mean. The standard deviation of the experiments is between 7.21 and 6.01 Ohms. Similar centrality and dispersion of data from the experiments, which is depicted in the figure below, translates to repeatability of the data produced by the instrument. The repeatability in this context means that the dispersion of data from the

mean should be within an acceptable range, which is 5 % in this case. This result can be attributed tothe similarity in the operational conditions of the experiments. Thus, we were able to demonstrate and verify our system's reliability in registering consistent curves for various market ready electrodes, making our system a viable system for testing future newly fabricated electrodes and compare them with readily available electrodes.

The experiments ran under the same conditions and the results show similarity in terms of value and shape versus time. One criteria of assessing this similarity is to look at the standard deviations. As impedance is the only under-investigation variable for experiments, there is no need to calculate and compare the coefficient of variables , and the standard deviation comparisons suffices. This is due to the fact that the unit of all variables in different experiments is the same and there is no need for a unitless tool (coefficient of variables) to compare the results of each experiment.

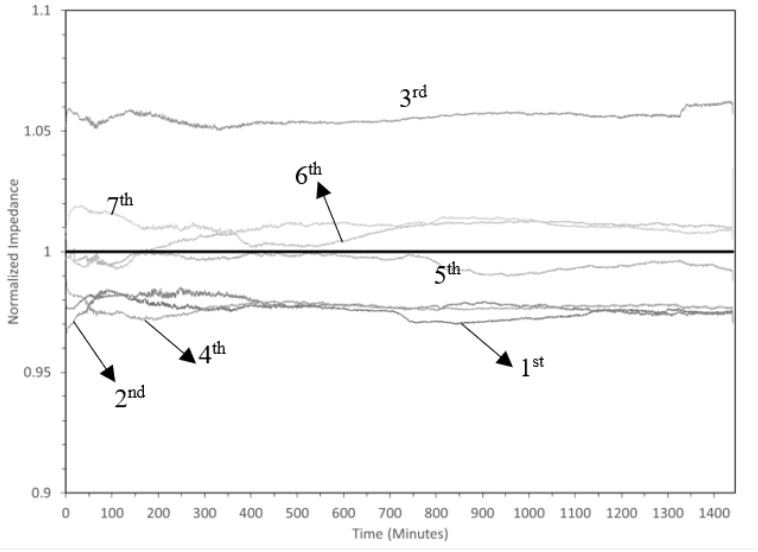

Figure 26: Normalized curved relative to the mean for the seven experiments

Figure 27 illustrates the normalized curve to their initial values for the seven experiments. As was observed in Figure 24, the starting point of experiments varied. This might have been because of human error at the stage of preparing the setup to run experiments. To normalize that effect, every data point on each curve was divided to the initial value of that experiment, as shown in Figure 27. In this figure, the shapes and trends are the same as Figure 24, except for the third experiment. The rest of the experiments were close enough to each other to be considered as illustrating the repeatability of the data.

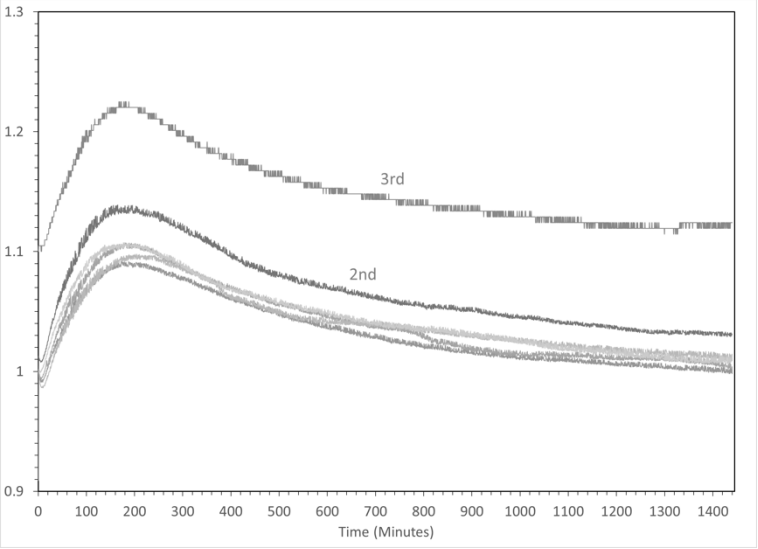

Figure 27: Normalized curve relative to the initial value of each experiment for the seven experiments

Figure 28 shows the local mean average of all experiments over the entire runtime. This figure was created by calculating the average of seven data points each time the LCR machine acquired data for all 2880 datasets. The figure shows a similar trend as each of the datasets shown before. In this context, the local average refers to the average of all data points each time the machine acquired data. Furthermore, Table 8 provides descriptive

statistics for the local mean of all seven experiments. The mean of the means and the standard deviation were used to apply the normal destribution empirical rule.

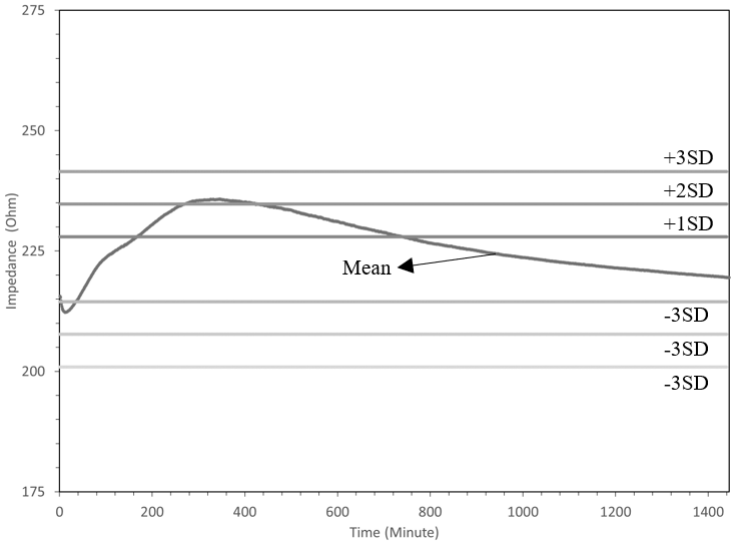

Figure 28: Impedance over time - local average of all experiments

Table 8: Descriptive statistics for the mean of the seven experiments

Mean	221.21
Standard Error	0.13
Median	218.94
Mode	234.86
Standard Deviation	6.76
Sample Variance	45.72
Kurtosis	-0.66
Skewness	0.78
Range	23.54
Minimum	212.27
Maximum	235.81
Sum	637090.91
Count	2880.00
Largest	235.81
Smallest	212.27
Confidence Level (95.0%)	0.25

Based on Table 9, two out of three criteria for the empirical rule were met within the mean of the means dataset. Based on the calculations presented in Table 9, 99% and 100% of the data points are within two and three standard deviations from the mean, respectively. Although 68% of the data points must be within one standard deviation from the mean, the resultant 59.4% is still acceptable considering the other two criteria results. Overall, based on the empirical rule analysis for the normal distributions, the mean curve of seven experiments was considered a normal distribution.

Table 9: Normal distribution empirical rule analysis for the mean of the means

Standard Deviation range from the mean	Actual number of Data within the specified range of the mean	Empirical Rule	Actual percentage of the data set	The actual number of data within the range	Result (YES=within the range; NO= out of the range)
1SD	1710	68.0%	59.4%	1958.4	NO
2SD	2852	95.0%	99.0%	2736	YES
3SD	2880	99.7%	100.0%	2871.36	YES

Figure 29 shows the difference between the local average and the median range of all data over the entire runtime. For this figure, the median of each dataset was specified. Then, the difference between the median and the local average was calculated. This procedure was repeated for all 2880 datasets. The resultant maximum and minimum of all the calculations were determined. Subsequently, the range between the maximum and minimum was calculated and divided in half. This figure was obtained by adding and subtracting the result from the local averages. The figure shows almost a stable range over the entire run time.

This is another piece of evidence that all the experiments followed a similar trend within a semi-constant distance.

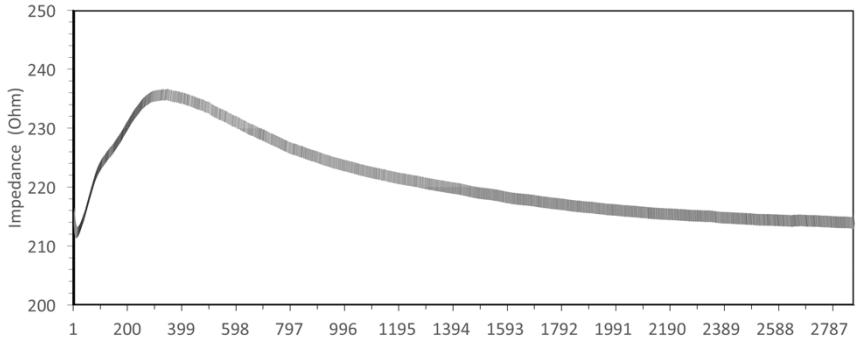

Figure 29: Average-median range difference fluctuation over time

Figure 30 shows the difference between the local median and the local average of all datasets. Median is a basic statistical tool that gives us a sense of centrality of all data. However, it does not consider the skewness of the data. Whereas the mean considers the skewness and gives us a sense of centrality. Observing how far they are from each other over the entire run time is another way to observe how close the data are generated over time. The results show that this difference was changed between 2.04 and 3.98 Ohms. The significance level was again considered to be 5%. This means that if the difference between the local median and the local average of all datasets remains within 5% deviation from the mean; then, the repeatability of trends in all experiments is acceptable. However, regardless of spontaneous change at the beginning, this range mostly revolved around 3 Ohms. Considering 221.21 Ohms, the mean of the means over the entire runtime, the 3 Ohms would be a 1.4% diversion from the average. This low range of fluctuation can be

considered evidence that the datasets from the seven experiments followed a similar pattern by keeping almost the same distance from each other over time. These two last figures show the deviation or edges variations from the average over time and help to illustrate how far the edges will go over time.

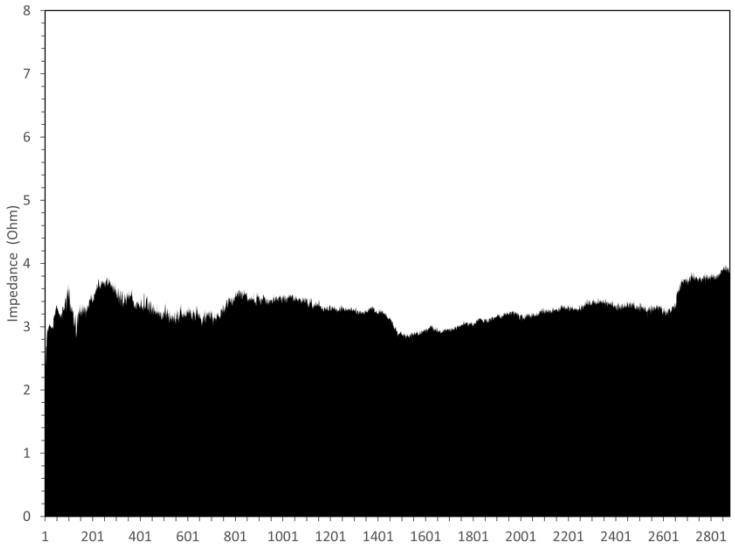

Figure 30: Average-median difference fluctuation over time

Stainless steel electrode was selected to find an answer for the following question: Do the observed fluctuations in the resultant impedances originate from the electrode properties and structure or from the electrochemical cell (the instrument) itself? To find an answer for that question, an experiment was run with a stainless steel electrode.

Stainless steel was chosen because of its durability and resistivity against corrosiveness. It has been suggested to use a noble metal; however, the lack of accessibility to such material led the current research team to use an alternative with similar properties. Resistivity to oxidation and corrosion in moist air is among noble metals' top properties. Likewise,

stainless steel has the same properties in terms of resistivity and corrosiveness. Considering the resource limitations in the laboratory, a stainless steel electrode was chosen for the current research.

Figure 31 illustrates the impedance over the entire run time for the stainless steel electrode at 4, 10, 30, 60, 90, and 120 Hz. It can be observed that all curves follow a relatively flat line over time. It seems that the lower the frequency, the higher the tiny fluctuations in the frequency, as can be seen for the 4 Hz associated curve. The objective at this point is to investigate whether at least 95% of the data revolve around the mean, leading the data to fit into a normal distribution model. Therefore, the normal distribution empirical rule was applied for all curves at various frequencies.

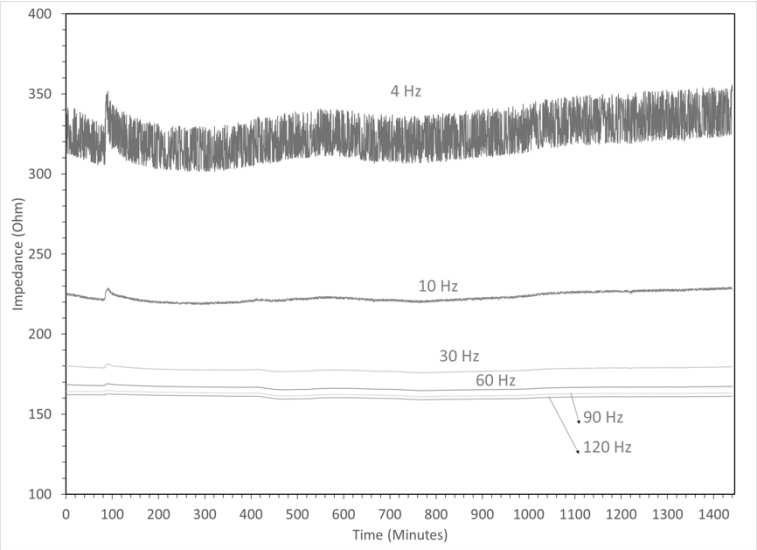

Figure 31: Impedance over time for stainless steel electrode at 4, 10, 30, 60, 90, and 120 Hz

Figure 32 shows the correlation between the impedance and frequency. The figure determines that the higher the frequency, the lower the impedance. By looking at the

equivalent circuit model (Figure 1) for the current research, it can be understood that the instrument is more capacitive in nature. Additionally, Equation 4 indicates an indirect correlation between the frequency and the impedance, which is in line with the observed trends in the figures. Additionally, the three curves in Figure 32 follow the same patten within a proximity for 30 seconds, 12 hours, and 24 hours after the start of the experiment. As time went on, the impedance stayed the same at the beginning, middle, and the end.

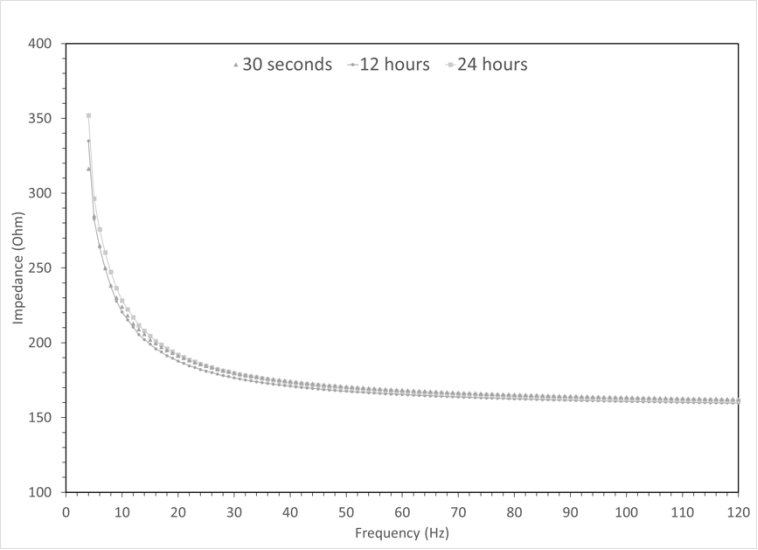

Figure 32: Impedance frequency dependency (stainless steel electrode) after 30 seconds, 12, and 24 hours

Table 10 presents the descriptive statistics for the impedance over time curves at 4, 10, 30, 60, 90, and 120 Hz. Using data, the trend, and properties of impedance at various frequencies can be interpreted. By looking at the skewness and kurtosis, the data at all frequencies seems to be normally distributed; that is, most of the data points at each frequency are close enough to their associated mean. The standard deviation shows the variability of the data. It can be understood from the standard deviation trend that the lower the frequency, the higher the standard deviation. Although all cases have a relatively low

value for their standard deviation, the impedance shows more variability at low frequencies. Furthermore, the mean and median at all frequencies are almost the same. This can be another sign of a normally distributed dataset.

Table 10 is to present the relationship between the frequency and the impedance and how it changes. It shows the importance of setting the standard requirement at the lowest possible frequency, even lower than 10 Hz. The 10 Hz frequency is the benchmark for experiments based on the ANSI/AAMI standard. The results of data acquisition at various frequencies are presented here both in descriptive statistics and multiple figures to show the relationship between the impedance and frequency.

Table 10: Descriptive statistics for the stainless steel electrode

Statistical Tool	**4 Hz**	**10 Hz**	**30 Hz**	**60 Hz**	**90 Hz**	**120 Hz**
Mean	324.84	223.16	177.91	166.48	162.62	160.64
Standard Error	0.23	0.05	0.02	0.02	0.02	0.02
Median	324.23	222.38	177.72	166.79	162.84	160.83
Mode	334.21	222.50	177.54	166.91	162.92	160.89
Standard Deviation	12.24	2.82	1.12	0.98	0.95	0.94
Sample Variance	149.77	7.98	1.25	0.95	0.90	0.88
Kurtosis	-0.79	-1.05	-0.85	-0.78	-0.91	-0.99
Skewness	0.24	0.44	0.15	0.06	0.09	0.12
Range	53.99	10.90	5.51	4.36	3.91	3.67
Minimum	301.69	218.50	175.77	164.67	160.92	159.01
Maximum	355.68	229.40	181.27	169.03	164.83	162.68
Sum	935547	642690	512387	479471	468332	462648
Count	2880.00	2880.00	2880.00	2880.00	2880.00	2880.00
Largest (1)	355.68	229.40	181.27	169.03	164.83	162.68
Smallest (1)	301.69	218.50	175.77	164.67	160.92	159.01
Confidence Level (95.0%)	0.45	0.10	0.04	0.04	0.03	0.03

The necessary distances from the mean were calculated using the standard deviation, mean, and the normal distribution empirical rule. These distances equal one, two and three

standard deviations from the mean value. Subsequently, the expected actual number of data within the specified range of the mean, the actual number of data within the range, and the actual percentage of the data within the range were calculated. Table 11 to Table 16 present the calculations associated with the normal distribution empirical rule. By looking at these tables, it can be concluded that all curves at all frequencies followed the normal distribution model. This means that at least 95% of all data points at each frequency were close to the mean. Considering the primary objective of this section of the current research, the results are aligned with the objective, and the electrochemical cell of the instrument provides a stable ion exchange environment over a long run time (about 31 hours).

Additionally, Figure 33 to Figure 38 illustrate the empirical rule associated ranges around the mean at each frequency for the stainless steel electrode.

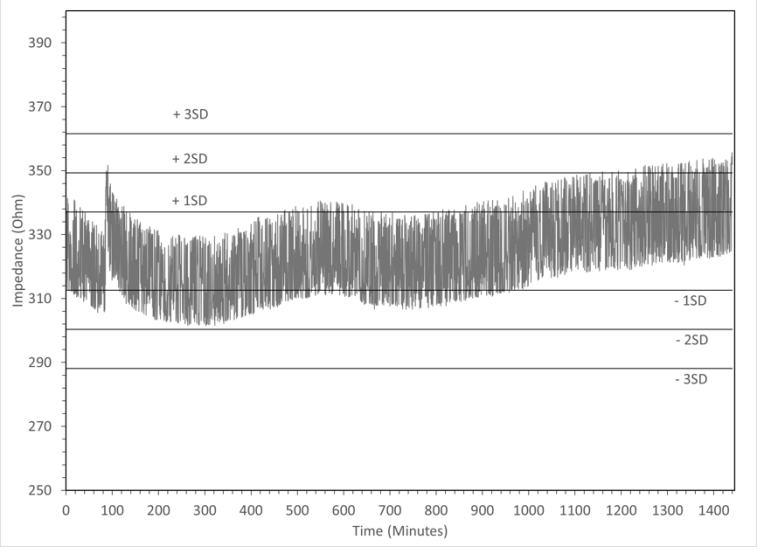

Figure 33: Impedance over time for stainless steel electrode at 4 Hz

Table 11: Normal distribution empirical rule analysis for the stainless steel electrode at 4 Hz

Standard Deviation range from the mean	The expected actual number of data withing the specified range of the mean	Empirical rule	Actual percentage of the data set	The actual number of data within the range	Result (YES=within the range; NO= out of the range)
1SD	1815	0.68	63.0%	1958.4	NO
2SD	2805	0.95	97.4%	2736	YES
3SD	2880	0.997	100.0%	2871.36	YES

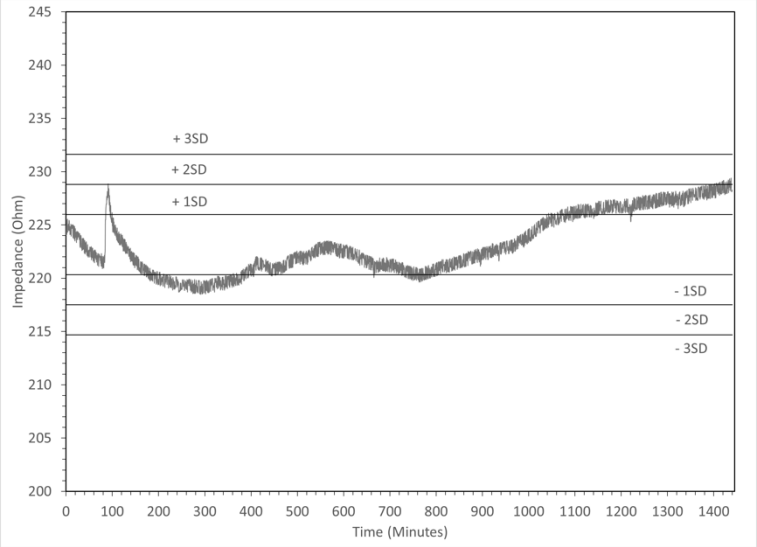

Figure 34: Impedance over time for stainless steel electrode at 10 Hz

Table 12: Normal distribution empirical rule analysis for the stainless steel electrode at 10 Hz

Standard Deviation range from the mean	The expected actual number of Data withing the specified range of the mean	Empirical Rule	Actual percentage of the data set	The actual number of data within the range	Result (YES=within the range; NO= out of the range)
1SD	1703	0.68	59.1%	1958.4	NO
2SD	2851	0.95	99.0%	2736	YES
3SD	2880	0.997	100.0%	2871.36	YES

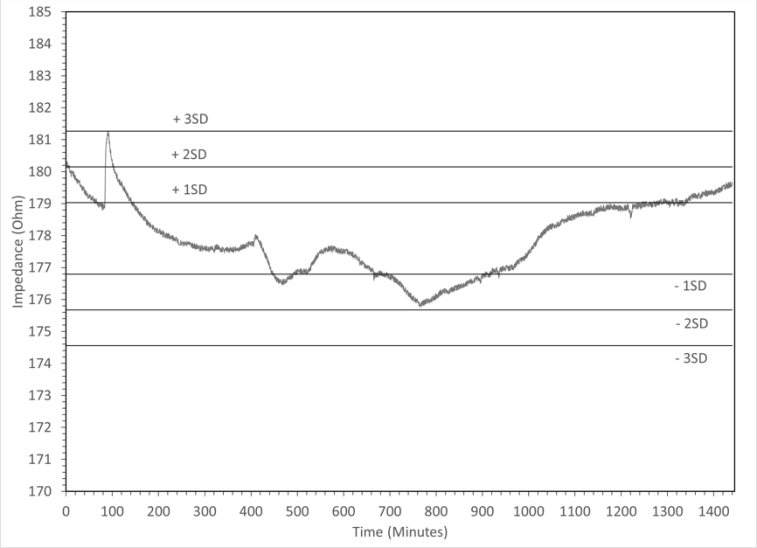

Figure 35: Impedance over time for stainless steel electrode at 30 Hz

Table 13: Normal distribution empirical rule analysis for the stainless steel electrode at 30 Hz

Standard Deviation range from the mean	The expected actual number of Data withing the specified range of the mean	Empirical Rule	Actual percentage of the data set	The actual number of data within the range	Result (YES=within the range; NO= out of the range)
1SD	1790	0.68	62.2%	1958.4	NO
2SD	2835	0.95	98.4%	2736	YES
3SD	2879	0.997	100.0%	2871.36	YES

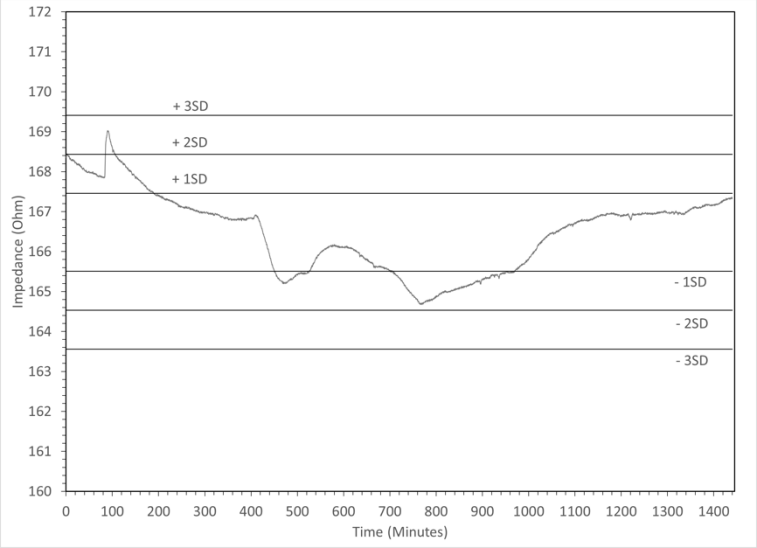

Figure 36: Impedance over time for stainless steel electrode at 60 Hz

Table 14: Normal distribution empirical rule analysis for the stainless steel electrode at 60 Hz

Standard Deviation range from the mean	The expected actual number of Data withing the specified range of the mean	Empirical Rule	Actual percentage of the data set	The actual number of data within the range	Result (YES=within the range; NO= out of the range)
1SD	1816	0.68	63.1%	1958.4	NO
2SD	2836	0.95	98.5%	2736	YES
3SD	2880	0.997	100.0%	2871.36	YES

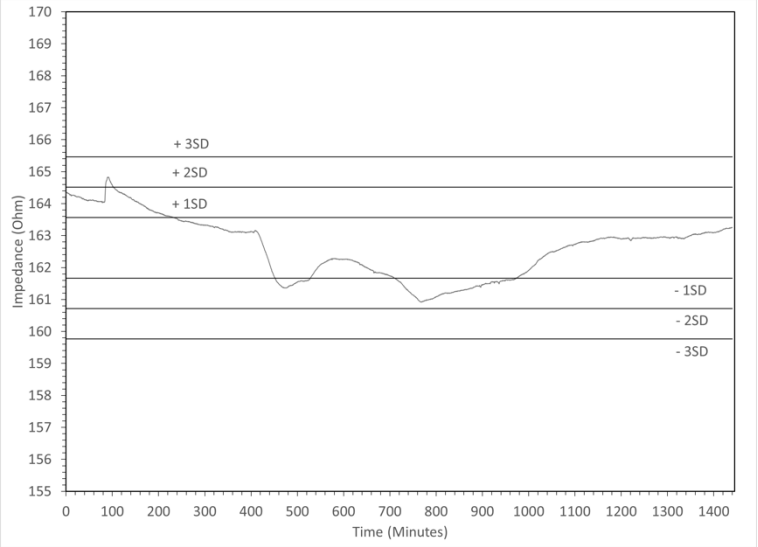

Figure 37: Impedance over time for stainless steel electrode at 90 Hz

Table 15: Normal distribution empirical rule analysis for the stainless steel electrode at 90 Hz

Standard Deviation range from the mean	The expected actual number of Data withing the specified range of the mean	Empirical Rule	Actual percentage of the data set	The actual number of data within the range	Result (YES=within the range; NO= out of the range)
1SD	1740	0.68	60%	1958.4	NO
2SD	2846	0.95	99%	2736	YES
3SD	2880	0.997	100%	2871.36	YES

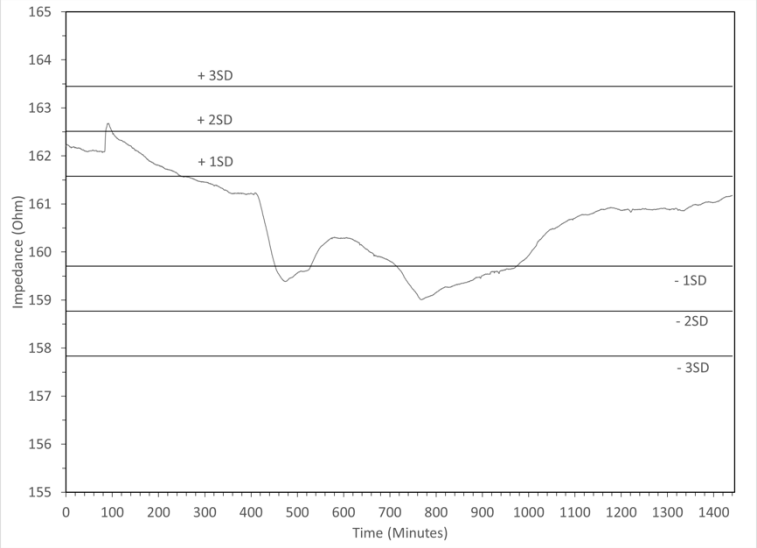

Figure 38: Impedance over time for stainless steel electrode at 120 Hz

Table 16: Normal distribution empirical rule analysis for the stainless steel electrode at 120 Hz

Standard Deviation range from the mean	The expected actual number of Data withing the specified range of the mean	Empirical Rule	Actual percentage of the data set	The actual number of data within the range	Result (YES=within the range; NO= out of the range)
1SD	1710	0.68	59.4%	1958.4	NO
2SD	2852	0.95	99.0%	2736	YES
3SD	2880	0.997	100.0%	2871.36	YES

The verification process and obtaining the local average of all experiments were done to conduct a comparative analysis between various electrodes. Figure 39 shows the impedance versus frequency over time for 2248-50 3M RedDot sponge electrode. It can be observed that the higher the frequency, the lower the impedance. The bottom edge of the data cloud shows the impedance at 120 Hz. By approaching the upper edge of the data cloud, the frequency decreases with a 1 Hz unit reduction to reach 4 Hz. As was mentioned earlier, ECG is a low-range frequency biopotential; therefore, setting up testing procedures for electrodes at low frequencies seems essential, considering the dependency of the impedance on the frequency.

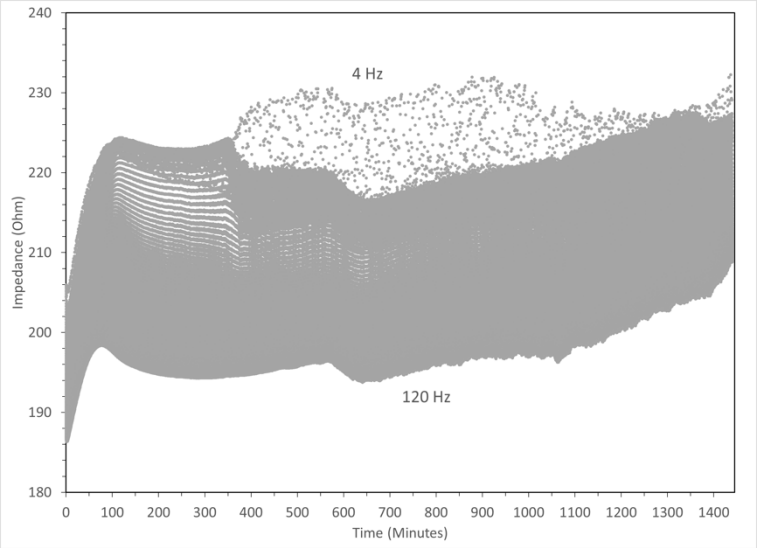

Figure 39: Impedance frequency dependency over time - 2248-50 3M RedDot sponge electrode

Figure 40 to Figure 45 illustrates the correlation between the impedance and frequency for the four chosen electrodes. These figures show the correlation at 30 seconds, 12 hours, and 24 hours after experiments started. All figures describe an indirect correlation between impedance and frequency. In other words, the higher the frequency, the lower the impedance. By looking at the equivalent circuit model (Figure 1) for the current research, it can be understood that the instrument is more capacitive in nature. Additionally, Equation 4 indicates an indirect correlation between the frequency and the impedance, which is in line with the observed trends in the figures.

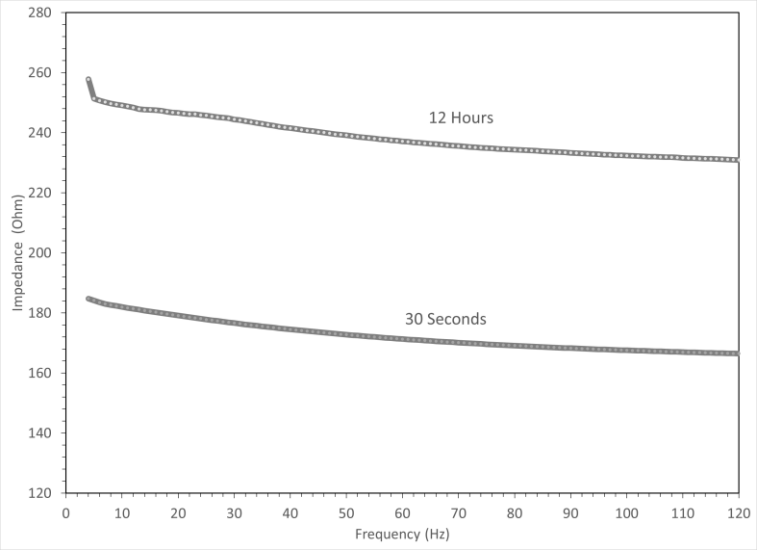

Figure 40: Impedance frequency dependency - 2249.50 sponge electrode - 30 seconds and 12 hours

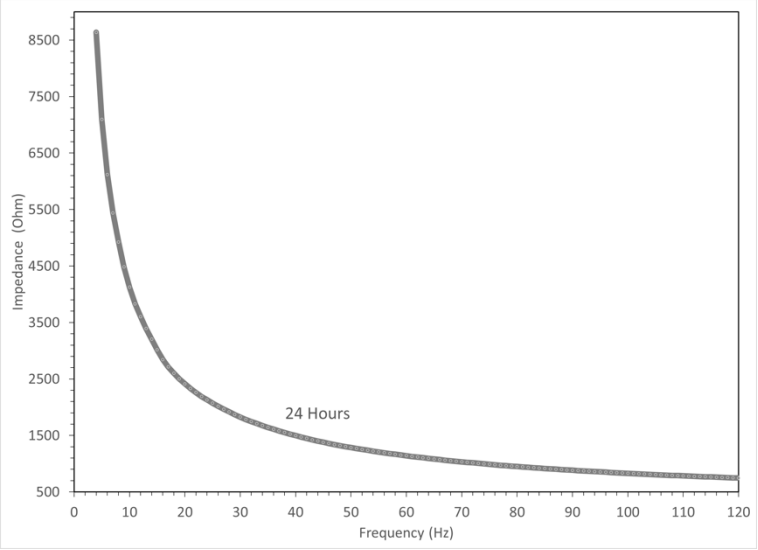

Figure 41: Impedance frequency dependency – 2249.50 sponge electrode - 24 hours

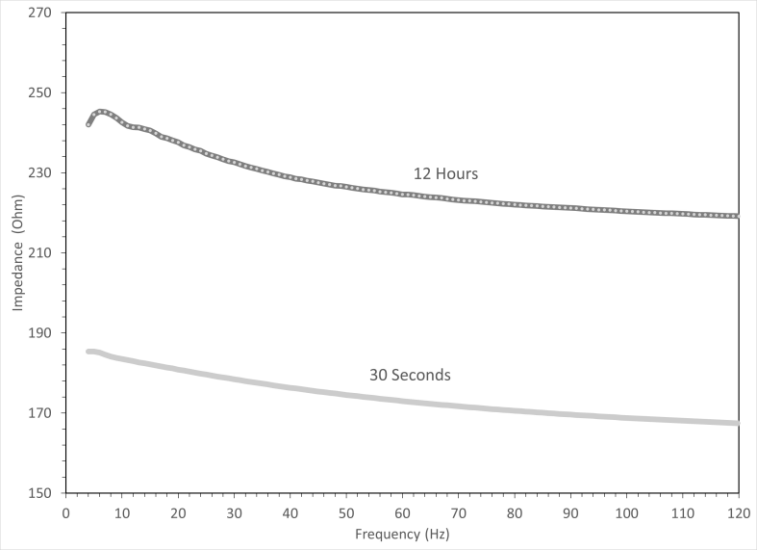

Figure 42: Impedance frequency dependency - 2231 sponge electrode - 30 seconds and 12 hours

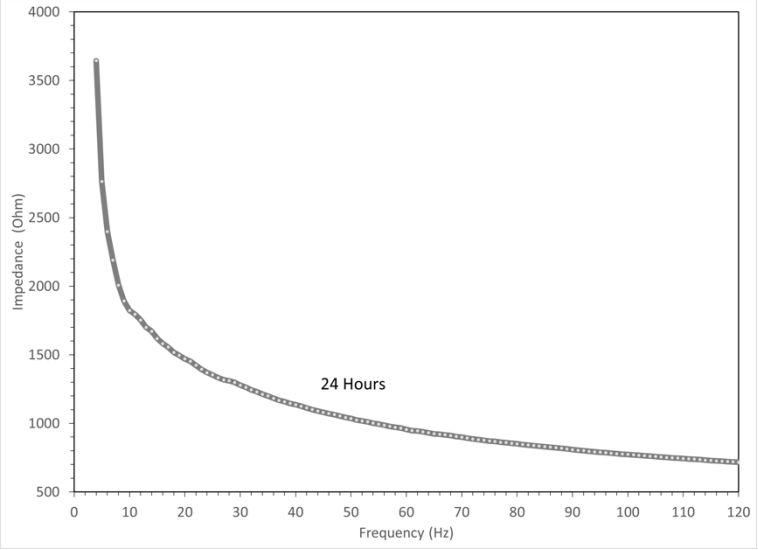

Figure 43: Impedance frequency dependency - 2231 sponge electrode - 24 hours

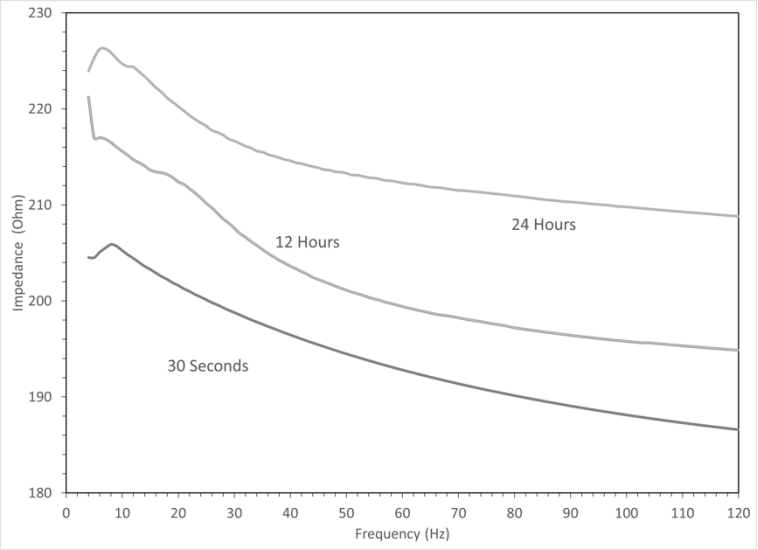

Figure 44: Impedance frequency dependency – 2249.50 sponge electrode - 30 seconds, 12 and 24 hours

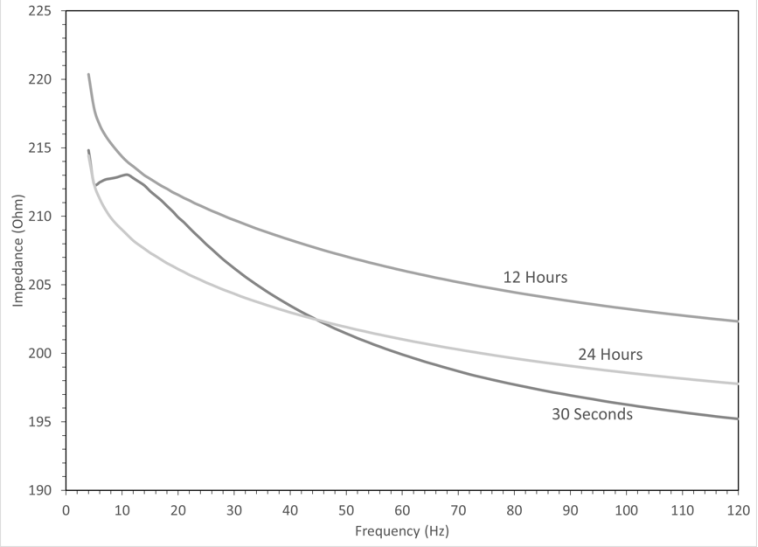

Figure 45: Impedance frequency dependency – 2579 hydrogel electrode - 30 seconds, 12 and 24 hours

Table 17 and Table 18 show the results of the F-test for the populations of 2880, and a sample populations of 1000 datapoints of both AgCl and stainless steel electrodes. The dataset for the AgCl electrode is the mean of all seven experiments to reflect all variabilities in the experiments. The population is the result of all datapoints acquired over the entire run time. The sample population consists of the last 1000 datapoints from the associated experiments. The reason for choosing the final datapoints is the observable stability in both electrode types. The significance level for both tests is 5%. The null hypothesis for these tests is "There is no difference between the variance of both electrodes." The alternative hypothesis is "Ag/AgCl electrode has a higher variance for impedance compared to stainless steel electrode."

If $P>0.05$, the null hypothesis cannot be rejected. On the other hand, if $P<0.05$, the null hypothesis can be rejected and the alternative hypothesis is correct. In this case, in both tests, P is much lower than 0.05 which means that the null hypothesis is rejected, and the alternative hypothesis is correct. Likely, the Ag/AgCl electrode has a higher variance for impedance compared to stainless steel electrode. This means that the instrument can show the difference between different types of electrodes.

Table 17: F-test results - for the populations of 2880 datapoints (AgCl and stainless steel electrodes)

Statistical parameter/tool	AgCl	SS
Mean	224.51	223.16
Variance	46.04	7.98
Observations	2880	2880
df	2879	2879
F	5.77	
P(F<=f) one-tail	0.00E+00	
F Critical one-tail	1.06	

Table 18: F-test results - for a sample populations of 1000 datapoints (AgCl and stainless-steel electrodes)

Statistical parameter/tool	AgCl	SS
Mean	226.38	209.48
Variance	2.57	0.28
Observations	1000.00	1000.00
df	999.00	999.00
F	9.26	
P(F<=f) one-tail	4.3342E-229	
F Critical one-tail	1.11	

Figure 46 demonstrates the experiment results from four different electrodes, as mentioned in the previous chapter. Both 2231 and 2249.50 electrodes' impedance started to increase after almost 200 minutes from the start of their experiments. The electrode 2231 and 2249.50 reached the impedance value of 3642.4 Ohm (Figure 47) and 337 Ohm at the end of their entire runtime, respectively. Electrode 2248.50 showed a similar performance over the runtime period with no significant difference from the electrode 2570 (hydrogel). On the other hand, at the beginning of the experiments, electrodes 2231 and 2249.50 resulted in having almost 16% lower impedance compared to the baseline. This trend continued until about 25 minutes after the start of the experiments.

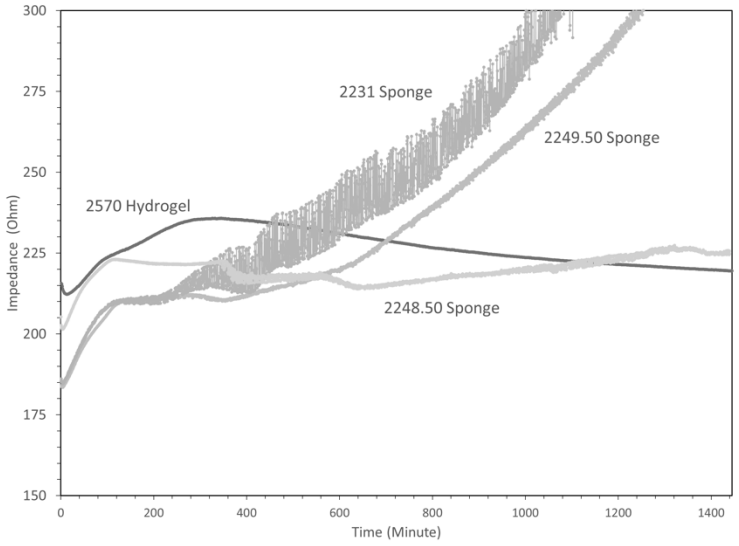

Figure 46: Impedance comparison over time for different medical electrodes with vertical axis range limit

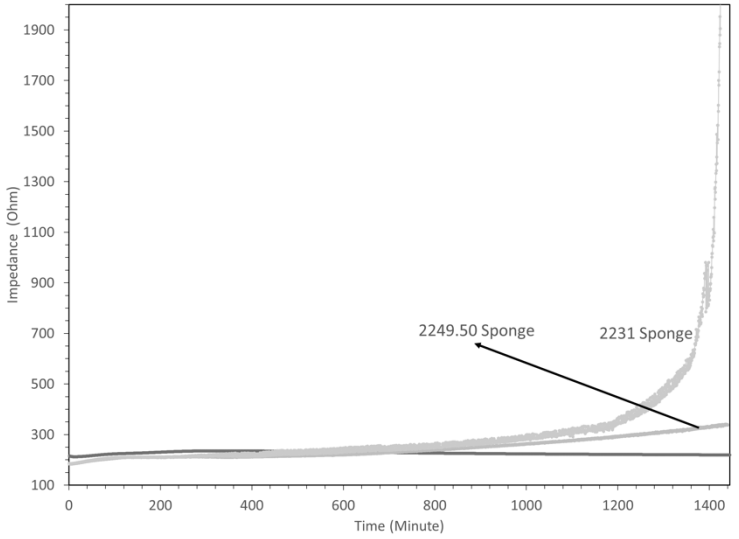

Figure 47: Impedance comparison over time for different medical electrodes with no axis limitation

Considering all results, one can understand that for short-term ECG monitoring, electrodes 2231 and 2249.50 would be the better candidates in terms of only electrical performance. Impedance is a barrier in signal acquisition from the body. The lower the impedance, the

easier the signal acquisition process. These two electrodes showed a relatively lower ranges of impedance for a short period of time (less than 30 minutes). Although all results within the first 30 minutes of the experiments are within the threshold (2000 Ohm) mentioned by the standard, it would be reasonable to choose the one with the lowest impedance if other factors like the price and adhesive patch matches the demand requirements.

The author should emphasize that this discussion is only about the impedance of the ECG medical electrode as one of the significant electrical performance parameters. Choosing the right electrode requires more investigation into other factors, including the adhesive patch, labelling, safety, price, and comfort level. On the other hand, considering all results, one can understand that for long-term ECG monitoring, electrodes 2570 and 2248.50 would be the better candidates for only electrical performance.

Figure 48 and Figure 49 show the observed conditions of the hydrogel electrode and the membrane after the experiment. It could be observed that the hydrogel was more liquid relative to the original status which was more solid. The membrane was observed to be fully wet and saturated with electrolyte after removing the electrodes. It should be noted that there was no observable difference between the beginning of the experiment and after the experiment for the sponge electrodes. However, by touching the sponge part of the electrodes, the sponge seemed to be drier after experiments. The observations were aligned with the manufacturers claim that the electrodes should not be kept out of the packages more than 30 days because they will dry out (Figure 50).

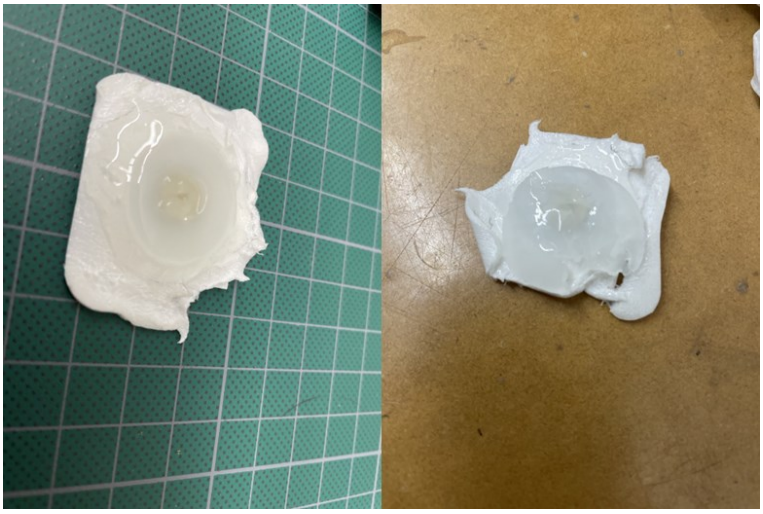

Figure 48: Hydrogel Electrode (2570) after the experiment

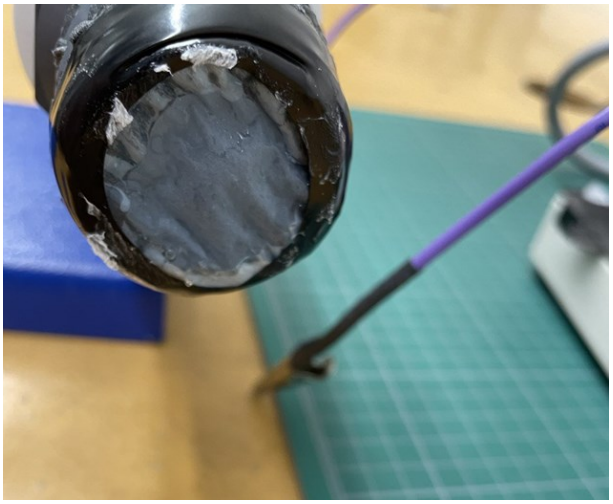

Figure 49: Membrane after the experiment

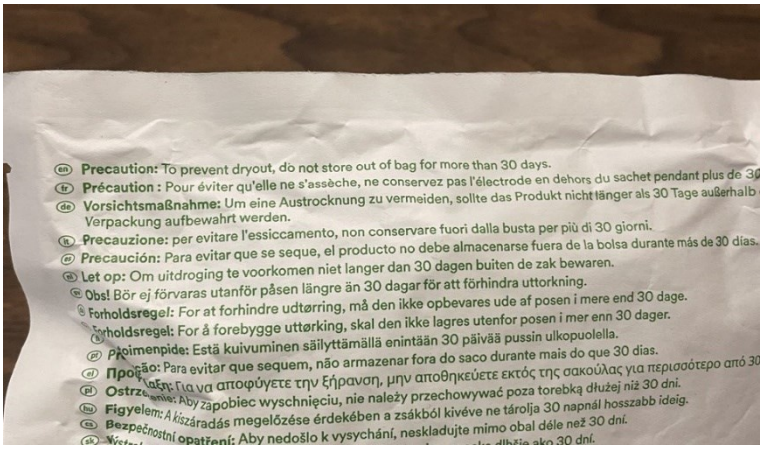

Figure 50: Manufacturer's description (3M) - "To prevent dry out, do not store out of the bag more than 30 days"

Table 19 shows the manufacturer's descriptions for four selected electrodes. Each of these electrodes seems to be for a specific type of application. Their patch structure is different, which might lead to different resistance when the gel dries out. Their sponge might also be another reason for the resultant differences in electrical performance. For instance, electrode 2231 is considered a diaphoretic monitoring electrode. This type of electrode is suitable for people with abnormal sweating in relation to their environment and activity level. This seems to be aligned with the skyrocketing electrical performance (Figure 47) of the electrode over the entire run time since no extra electrode gel or electrolyte was added.

Table 19: Manufacturer's descriptions for four selected electrodes

Electrode Model	Description
3M RedDot 2570	Radiolucent Monitoring Electrode with Foam Tape, Sticky Gel and Abrader Pad
3M RedDot 2249.50	Monitoring Electrode with Micropore Tape and Solid Gel
3M RedDot 2231	Diaphoretic Monitoring Electrode with Soft Cloth Tape and Solid Gel
3M RedDot 2248.50	Monitoring Electrode with Micropore Tape and Solid Gel

The other advantage of making such comparative figures is to improve the quality of electrodes under development in research laboratories. More specifically, by having the ANSI/AAMI standard requirements and limitations about the electrical performance, the target can be set for the research team to achieve by manipulating various impactful parameters in the electrode performance. Consequently, this makes the electrode fabrication procedure more time- and cost-effective.

4.2.Validation

To validate the instrument, similar prior works were reviewed as another significant step in the current research. The most similar research was chosen to check the current research results. The selected research was conducted by a group of researchers at Heriot-Watt University in the United Kingdom (An & Stylios, 2018). They made a similar instrument to test hybrid textile electrodes for ECG measurements. The testing setup in their research was aligned vertically, whereas the instrument in the current research was aligned horizontally. The horizontal orientation was chosen to eliminate the effect of static fluid pressure differences on both membranes. The static pressure inside the chamber can be an

effective parameter in the final impedance measurement. Thus, keeping this parameter the same throughout all experiments made the instrument results more reliable. Additionally, unlike the prior work, a venting system was considered in the current instrument to allow the user to inject fluids and apply pressure head. Other differences can be found in Table 20.

The electrodes on both sides were kept the same in the current research to comply with standards. Also, unlike the prior research, selecting the same electrodes on both sides of the chamber eliminated the DC bias effect from this parameter. The total original duration of the current research was 24 hours. The prior research was done within one hour. The longer runtime was chosen to investigate the impedance change and the electrode electrical performance, specifically when the patient must wear the electrodes for a day or two for ECG monitoring. The experiments' frequency range for the current research was chosen to be between 4 Hz to 120 Hz as a more exact simulation of the frequency generated by the physiological activities of the human heart and aligned with the standards electrical testing requirements. Figure 51 shows the setup from the prior research.

The results from both research projects show similar general trends; that is, the impedance is a frequency-dependent electrical parameter. Additionally, both research projects show that the higher the frequency, the lower the impedance. As time progresses in experiments, the impedance follows a more stable trend with minor changes in the value. Figure 52 and Figure 53 show the prior research results and the correlations between impedance, time, and frequency.

Table 20: Comparison between the current and prior research parameters of the testing setup (instrument)

Item	**Current Research**	**Prior Research** (An & Stylios, 2018)
Membrane	polyvinylidene fluoride (PVDF); 100 nm pore size	polyvinylidene fluoride (PVDF); 100 nm pore size
Chamber	Polyvinyl Chloride (PVC)	Polyvinyl Chloride (PVC)
Ionic Solution	NaCl 0.9% in deionized water	NaCl 0.9%
Electrode	Both electrodes on both sides were the same	A base Ag/AgCl electrode was used in all experiments on one side of the chamber.
LCR Meter	HIOKI General-Purpose LCR Meters IM 3536; Japan; frequency range DC, 4 Hz to 8 MHz	LCR-Bridge meter (HM8118, HAMEG instruments, Mainhausen, Germany)
Experiments Frequency Range	4 Hz to 120 Hz	20 Hz to 20 kHz
Room Temperature ℃	22 ± 5	20 ± 2
Relative Humidity %	40 ± 10	65 ± 2

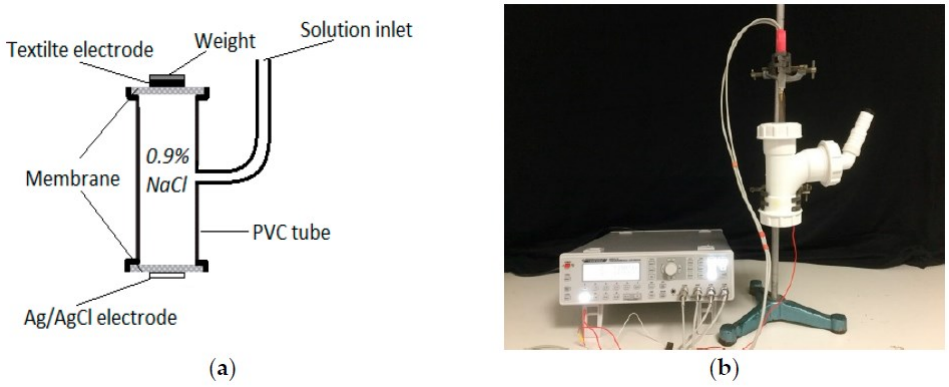

Figure 51: Skin-electrode impedance measurement on a skin dummy: (a) Skin dummy; (b) test setup (with permission as per the open access policy)

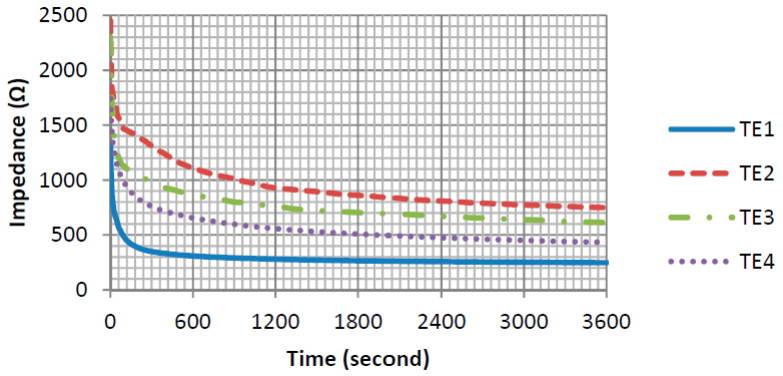

Figure 52: Skin-electrode impedance in 1 h (with permission as per the open access policy)

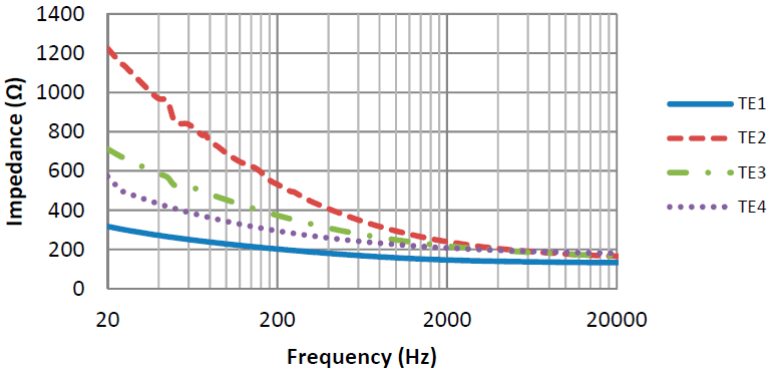

Figure 53: Skin-electrode impedance versus frequency (with permission as per the open access policy)

By comparing the seven experiments' results from the Ag/AgCl 2570 electrode, and the results presented in Figure 52 and Figure 53 from the prior research, the range of impedance for a silver chloride wet electrode are similar. The current research showed a mean impedance of 221 Ohms. Likely, the prior research shows a similar range of impedance after the stabilization of the electrodes. This reflects the validity of the data produced by the instrument.

Every instrument and instrumentation process has sources of errors, and there is no exception with the current experiments. They could be from human error in setting up the instrument and the preparation phase, or they may originate from the devices. Eliminating those possible errors will help the instrument's repeatability and reproducibility.

The current research was about the preliminary design, integration, and validation of an instrument as a simulated environment for the medical electrode electrical performance comparative analysis under human physiological conditions. These physiological conditions are ionic transfer environment, body temperature, body fluidic pressure, skin structure, sweat pH and composition, sweat secretion, and sweat ion concentration. The current attempt focused on the ionic transfer environment and the human heart frequency range. It is recommended that other parameters be investigated using the instrument.

Electrical performance is not just about impedance results; other electrical parameters need to be analyzed to provide a more comprehensive observation of the relative electrical performance of each electrode. However, it should be noted that impedance analysis is the crucial parameter to investigate in biopotential analysis. This is because impedance is the main barrier to transfer the charges coming from the organs in the human body to the signal receivers, e.g., ECG machines. It is recommended to tune the environmental conditions and other parameters to the exact ranges mentioned in the ANSI/AAMI standard and investigate the effect of various changing factors on electrical performance such as impedance.

Microscale studies of the interactions between the membrane, gel, and electrodes would provide a better and more in-depth understanding of how the instrument and the associated testing procedure create data and evaluate the electrode performance. Additionally,

simulating and characterizing the future upgraded instrument would be a fundamental approach to make a cost-effective way of observing the effect of different parameters on the electrical performance of electrodes.

Though it was mentioned in the ANSI/AAMI standard that measuring the impedance at 10 Hz frequency for time intervals less than an hour would be the acceptable approach, it is recommended to conduct the measurements from 0.1 Hz to 150 Hz over longer runtimes, e.g., 24 hours. It was observed from the experiments that the lower the frequency, the higher the fluctuations in the impedance measurements.

One of the associated problems with ECG electrodes is sweat secretion from human skin and its negative impact on both the measurements and the adhesive patch. It is recommended to study the effect of sweat secretion with various compositions and concentrations on the electrical performance of such electrodes. As another avenue for the current instrument, it seems that the instrument can be a good candidate for biochemical sensors. This capability needs more investigation to be done by the research team in the future.

Chapter 5 – Conclusions and Recommendations

5.1.Conclusions

The scope of the current research is to redesign, integrate, verify, and validate a preliminary testing setup based on the ANSI/AAMI standard for medical electrode qualification in research laboratories. The objective of the current work is to make sure the redesigned and integrated preliminary testing setup could be a good starting point to further invest time and money on leveraging the structure and performance of the setup. The significance level of success for the current attempt is to observe the verified and validated results from the testing setup. Additionally, the setup must be able to provide a stable ion exchange environment for targeted electrodes for investigation. The focus of the current research is on ECG as the targeted biopotential and the electrical performance as one of the critical factors to be studied. ECG was selected as it shows the overall condition and performance of a vital organ, the heart. Additionally, impedance was studied as a starting point for the electrical performance analysis of medical electrodes. Appropriate experiments were designed to verify results produced by the testing setup. The stability of data produced by the setup was investigated using a stainless steel electrode. Numerous tests and analysis, including a hypothesis test, Dixon's Q test, and normal distribution empirical rule analysis were performed on resultant data from various electrodes. The results of the electrical performance of electrodes were compared together to draw conclusions.

It was observed from the experiments that the lower the frequency, the higher the fluctuations in the impedance measurements. It could be concluded that all curves at all frequencies follow the normal distribution model. This means that at least 95% of all data points at each frequency are close to the mean. The results are aligned with the objective,

and the electrochemical cell of the instrument provides a stable ion exchange environment over a long run time (about 31 hours) as well.

It was observed that the hydrogel was more liquid relative to the original status, which was more solid. The membrane was observed to be fully wet and saturated with electrolyte after removing the electrodes. It should be noted that there was no observable difference between the beginning and after the experiment for the sponge electrodes. However, by touching the sponge part of electrodes, the sponge seemed to be drier after the experiments. The observations were aligned with the manufacturer's claim that the electrodes should not be kept out of the packages more than 30 days because they will dry out.

The current research showed a mean impedance of 221 Ohms. Likely, the prior research shows a similar range of impedance after the stabilization of the electrodes. This reflects the validity of the data produced by the instrument. F-test results demonstrated the capability of the instrument to distinguish the performance difference among various types of electrodes.

Based on the manufacturer's description on the product packages, electrode 2231 is considered a diaphoretic monitoring electrode. This type of electrode is suitable for people with abnormal sweating in relation to their environment and activity level. This seems to be aligned with the skyrocketing electrical performance of the electrode over the entire run time since no extra electrode gel or electrolyte was added.

Considering all results, for short-term ECG monitoring, electrodes 2231 (sponge) and 2249.50 (sponge) would be better candidates if only electrical performance were considered. It should be emphasized that this discussion is only about the impedance of the

ECG medical electrode as one of the significant electrical performance parameters. Choosing the right electrode requires more investigation into other factors, including the adhesive patch, labelling, safety, price, and comfort level. On the other hand, considering all results, for long-term ECG monitoring, electrodes 2570 (hydrogel) and 2248.50 (sponge) would be better candidates based on the same electrical performance criterion. Overall, the current work shows that the designed integrated preliminary testing setup is a good starting point to further invest resources develop the setup.

5.2.Recommendations

Though it was mentioned in the ANSI/AAMI standard that measuring the impedance at 10 Hz frequency for time intervals less than an hour would be the acceptable approach, it is recommended to conduct the measurements from 0.1 Hz to 150 Hz over longer runtimes, e.g., 24 hours, as a more exact simulation of the frequency generated by the physiological activities of the human heart and aligned with standard electrical testing requirements.

As other researchers were working in the same space and using the same equipment, running more experiments was not possible. As a result, it should be noted that more experiments are recommended to investigate the repeatability of data for the next versions of the instrument. Aside from the number of experiments, the same procedure, operator, equipment, environmental conditions, location, and item or unit under test must be accommodated to run repeatability tests.

One of the associated problems with the ECG electrodes is sweat secretion from human skin and its negative impact on both the measurements and the adhesive patch. It is recommended to study the effect of sweat secretion with various compositions and

concentrations on the electrical performance of such electrodes. Additionally, Microscale studies of the interactions between the membrane, gel, and electrodes would provide a better and more in-depth understanding of how the instrument and the associated testing procedure create data and evaluate the electrode performance.

It is recommended to tune the environmental conditions and other parameters to the exact ranges mentioned in the ANSI/AAMI standard and investigate the effect of various changing factors on the electrical performance such as impedance.

References

Acar, G., Ozturk, O., Golparvar, A. J., Elboshra, T. A., Böhringer, K., & Kaya Yapici, M. (2019). Wearable and flexible textile electrodes for biopotential signal monitoring: A review. *Electronics (Switzerland)*, *8*(5), 1–25. https://doi.org/10.3390/electronics8050479

Albulbul, A. (2016). Evaluating major electrode types for idle biological signal measurements for modern medical technology. *Bioengineering*, *3*(3). https://doi.org/10.3390/bioengineering3030020

An, X., & Stylios, G. K. (2018). A hybrid textile electrode for electrocardiogram (ECG) measurement and motion tracking. *Materials*, *11*(10). https://doi.org/10.3390/ma11101887

ANSI/AAMi. (2020). *Disposable ECG Electrodes: American National Standard, ANSI/AAMI EC12:2000.*

Based, T. E., & Lectrodes, E. C. G. E. (2022). *Electrode-Skin Impedance Characterization of Textile-Based ECG Electrodes*. 1–2. http://hdl.handle.net/1854/LU-8756728

Bronzino, E. J. D. (2000). *Neuman, M. R. "Biopotential Electrodes."*

Cambridge University Press. (2022). *Cambridge Dictionary*. https://dictionary.cambridge.org/dictionary/english/reliability

Dong, J., Wang, D., Peng, Y., Zhang, C., Lai, F., He, G., Ma, P., Dong, W., Huang, Y., Parkin, I. P., & Liu, T. (2022). Ultra-stretchable and superhydrophobic textile-based bioelectrodes for robust self-cleaning and personal health monitoring. *Nano Energy*, *97*, 107160. https://doi.org/https://doi.org/10.1016/j.nanoen.2022.107160

Eskandarian, L., Toossi, A., Nassif, F., Golmohammadi Rostami, S., Ni, S., Mahnam, A., Alizadeh Meghrazi, M., Takarada, W., Kikutani, T., & Naguib, H. E. (2022). 3D-Knit Dry Electrodes using Conductive Elastomeric Fibers for Long-Term Continuous Electrophysiological Monitoring. *Advanced Materials Technologies*, *2101572*, 1–13. https://doi.org/10.1002/admt.202101572

Frost, J. (2022). *Empirical Rule: Definition & Formula*. https://statisticsbyjim.com/probability/empirical-rule/

Fu, Y., Zhao, J., Dong, Y., & Wang, X. (2020). Dry electrodes for human bioelectrical signal monitoring. *Sensors (Switzerland)*, *20*(13), 1–30. https://doi.org/10.3390/s20133651

Gross, C. A., & Roppel, T. A. (2012). Fundamentals of electrical engineering. *Fundamentals of Electrical Engineering*, 1–448. https://doi.org/10.1201/b11786

Ha, S., Kim, C., Wang, H., Chi, Y. M., Mercier, P. P., & Cauwenberghs, G. (2021). Low-power integrated circuits for wearable electrophysiology. *Wearable Sensors*, 163–199. https://doi.org/10.1016/B978-0-12-819246-7.00006-1

Healthwise Staff. (2021). *SA Node and AV Node*. https://myhealth.alberta.ca/Health/pages/conditions.aspx?hwid=sts14215&#:~:text=The SA (sinoatrial) node generates,the pacemaker of the heart

Heikenfeld, J., Jajack, A., Rogers, J., Gutruf, P., Tian, L., Pan, T., Li, R., Khine, M., Kim, J., Wang, J., & Kim, J. (2018). Wearable sensors: Modalities, challenges, and prospects. *Lab on a Chip*, *18*(2), 217–248. https://doi.org/10.1039/c7lc00914c

Hogan, R. (2018). *How to Perform a Repeatability Test for Estimating Uncertainty in Measuremen*. https://www.isobudgets.com/how-to-perform-a-repeatability-test/

Industrial Deegreasers. (2018). *The Benefits of an Acetone Cleaner*. Ecolink. https://ecolink.com/info/benefits-of-acetone-cleaner/#:~:text=Using Acetone as a Solvent,the surface of an item.

ISOPROPYL ALCOHOL AS A CLEANING AGENT. (2021). Sunrise Industrial Cleaners. https://www.sunriseindustrial.com/isopropyl-alcohol-as-a-cleaning-agent/#:~:text=Isopropyl alcohol is a potent,cell wall of an organism.

Kim, Y. K., Wang, H., & Mahmud, M. S. (2016). Wearable body sensor network for health care applications. *Smart Textiles and Their Applications*, 161–184. https://doi.org/10.1016/B978-0-08-100574-3.00009-6

Laboratory, U. B. T. (1979). *Development of Test Methods for Disposable Ecg Electrodes*.

Macay, A. (1963). *Chapter 10: Biopotential Signals*. 6. https://alanmacy.com/books/the-handbook-of-human-physiological-recording/chapter-10-biopotential-signals/

Macdonald, J. R. (1992). Impedance spectroscopy. *Annals of Biomedical Engineering*, *20*(3), 289–305.

Madhu. (2020). *Difference Between Polarizable and Non Polarizable Electrode*. https://www.differencebetween.com/difference-between-polarizable-and-non-polarizable-electrode/

Maithani, Y., Singh, A., Mehta, B. R., & Singh, J. P. (2022). PEDOT: PSS treated cotton-based textile dry electrode for ECG sensing. *Materials Today: Proceedings*, *62*, 4052–4057. https://doi.org/https://doi.org/10.1016/j.matpr.2022.04.611

Malmivuo, J. (1995). Electric and Magnetic Measurement of the Electric Activity of the Heart. In *Bioelectromagnetism: Principles and Applications of Bioelectric and Biomagnetic Fields*.

Nigusse, A. B., Malengier, B., Mengistie, D. A., Tseghai, G. B., & Van Langenhove, L. (2020). Development of washable silver printed textile electrodes for long-term ECG monitoring. *Sensors (Switzerland)*, *20*(21), 1–16. https://doi.org/10.3390/s20216233

Oreggioni, J., Caputi, A. A., & Silveira, F. (2019). Biopotential monitoring. *Encyclopedia of Biomedical Engineering*, *1–3*, 296–304. https://doi.org/10.1016/B978-0-12-801238-3.64161-2

Park, S., & Jayaraman, S. (2021). *Chapter 1 - Wearables: Fundamentals, advancements, and a roadmap for the future* (E. B. T.-W. S. (Second E. Sazonov (Ed.); pp. 3–27). Academic Press. https://doi.org/https://doi.org/10.1016/B978-0-12-819246-7.00001-2

Priniotakis, G., Westbroek, P., Van Langenhove, L., & Kiekens, P. (2005). An experimental simulation of human body behaviour during sweat production measured at textile electrodes. *International Journal of Clothing Science and Technology*, *17*(3–4), 232–241. https://doi.org/10.1108/09556220510590939

Raschka, S. (2014). *Dixon's Q test for outlier identification*. https://sebastianraschka.com/Articles/2014_dixon_test.html

Rorabacher, D. B. (1991). Statistical Treatment for Rejection of Deviant Values: Critical Values of Dixon's "Q" Parameter and Related Subrange Ratios at the 95% Confidence Level. *Analytical Chemistry*, *63*(2), 139–146. https://doi.org/10.1021/ac00002a010

Saboo, R. (2017). *R&D: The backbone of innovation to compete with global standards*. The Economic Times. https://auto.economictimes.indiatimes.com/autologue/r-d-the-backbone-of-innovation-to-compete-with-global-standards/2650

Schauss, G. (2022). Wearable Textile Electrocardiogram Sport Bra for Real Time Health Monitoring [University of Colorado at Boulder PP - United States -- Colorado]. In *ProQuest Dissertations and Theses*. https://ezproxy.library.dal.ca/login?url=https://www.proquest.com/dissertations-theses/wearable-textile-electrocardiogram-sport-bra-real/docview/2678689414/se-2?accountid=10406

Sheppard, J. P., Barker, T. A., Ranasinghe, A. M., Clutton-Brock, T. H., Frenneaux, M. P., & Parkes, M. J. (2011). Does modifying electrode placement of the 12 lead ECG matter in healthy subjects? *International Journal of Cardiology*, *152*(2), 184–191. https://doi.org/https://doi.org/10.1016/j.ijcard.2010.07.013

Slurzberg, Morris; Osterheld, William, joint author. (1950). *Essentials of electricity for radio and television*. New York, McGraw-Hill.

Sun, Y., & Yu, X. B. (2016). Capacitive Biopotential Measurement for Electrophysiological Signal Acquisition: A Review. *IEEE Sensors Journal*, *16*(9), 2832–2853. https://doi.org/10.1109/JSEN.2016.2519392

Teferra, M. N., Hobbs, D. A., Clark, R. A., & Reynolds, K. J. (2022). Electronic-Textile 12-Lead Equivalent Diagnostic Electrocardiogram Based on the EASI Lead Placement. *IEEE Sensors Journal*, *22*(6), 5994–6001. https://doi.org/10.1109/JSEN.2022.3146454

Thakor, N. V. (2014). Biopotentials and Electrophysiology Measurement. *Measurement, Instrumentation, and Sensors Handbook*, 64-1-64–18. https://doi.org/10.1201/b15664-64

Tobias, A., Ballard, B. D., & Mohiuddin, S. S. (2022). *Physiology, Water Balance.*

Tronstad, C., Johnsen, G. K., Grimnes, S., & Martinsen, Ø. G. (2010). A study on electrode gels for skin conductance measurements. *Physiological Measurement*, *31*(10), 1395–1410. https://doi.org/10.1088/0967-3334/31/10/008

Wang, L., Pan, Y., He, D., Qian, L., Cao, X., He, B., & Li, J. (2022). Conductive Polyester Fabrics with High Washability as Electrocardiogram Textile Electrodes. *ACS Applied Polymer Materials*, *4*(2), 1440–1447. https://doi.org/10.1021/acsapm.1c01619

Werner, J. (2014). Electrocardiography. *Comprehensive Biomedical Physics*, *5*, 25–45. https://doi.org/10.1016/B978-0-444-53632-7.00507-4

Westbroek, P., Priniotakis, G., Palovuori, E., de Clerck, K., Van Langenhove, L., & Kiekens, P. (2006). Quality Control of Textile Electrodes by Electrochemical Impedance Spectroscopy. *Textile Research Journal*, *76*(2), 152–159. https://doi.org/10.1177/0040517506053911

Zhao, Jingjing, Deng, J., Liang, W., Zhao, L., Dong, Y., Wang, X., & Lin, L. (2022). Water-retentive, 3D knitted textile electrode for long-term and motion state bioelectrical signal acquisition. *Composites Science and Technology*, *227*, 109606. https://doi.org/https://doi.org/10.1016/j.compscitech.2022.109606

Zhao, Jun, Sclabassi, R. J., & Sun, M. (2005). Biopotential electrodes based on hydrogel. *Proceedings of the IEEE Annual Northeast Bioengineering Conference, NEBEC*, *C*, 69–70. https://doi.org/10.1109/nebc.2005.1431929

Appendix A: Permissions

AAMI
Advancing Safety in Health Technology

ELSEVIER LICENSE
TERMS AND CONDITIONS

Jul 27, 2022

This Agreement between Mr. Rez Ghasemi ("You") and Elsevier ("Elsevier") consists of your license details and the terms and conditions provided by Elsevier and Copyright Clearance Center.

License Number	5357180982567
License date	Jul 27, 2022
Licensed Content Publisher	Elsevier
Licensed Content Publication	International Journal of Cardiology
Licensed Content Title	Does modifying electrode placement of the 12 lead ECG matter in healthy subjects?
Licensed Content Author	James P. Sheppard,Thomas A. Barker,Aaron M. Ranasinghe,Thomas H. Clutton-Brock,Michael P. Frenneaux,Michael J. Parkes
Licensed Content Date	Oct 20, 2011
Licensed Content Volume	152
Licensed Content Issue	2
Licensed Content Pages	8
Start Page	184

End Page	191
Type of Use	reuse in a thesis/dissertation
Portion	figures/tables/illustrations
Number of figures/tables/illustrations	1
Format	both print and electronic
Are you the author of this Elsevier article?	No
Will you be translating?	No
Title	MEDICAL ELECTRODE QUALIFICATION: PRELIMINARY DESIGN, INTEGRATION, AND VALIDATION OF THE TESTING SETUP
Institution name	Dalhousie University
Expected presentation date	Aug 2022
Portions	Figure 1
Requestor Location	Mr. Rez Ghasemi 5206 Tobin St, 110 Apt Halifax, NS B3H1s2 Canada Attn: Dalhousie University
Publisher Tax ID	GB 494 6272 12
Total	0.00 CAD

Appendix B: List of Equations